Coonamessett Farm Foundation

Davis Bank East Survey

DRAFT- Final Report for Exempted Fishing Permit #23073

July 31, 2026

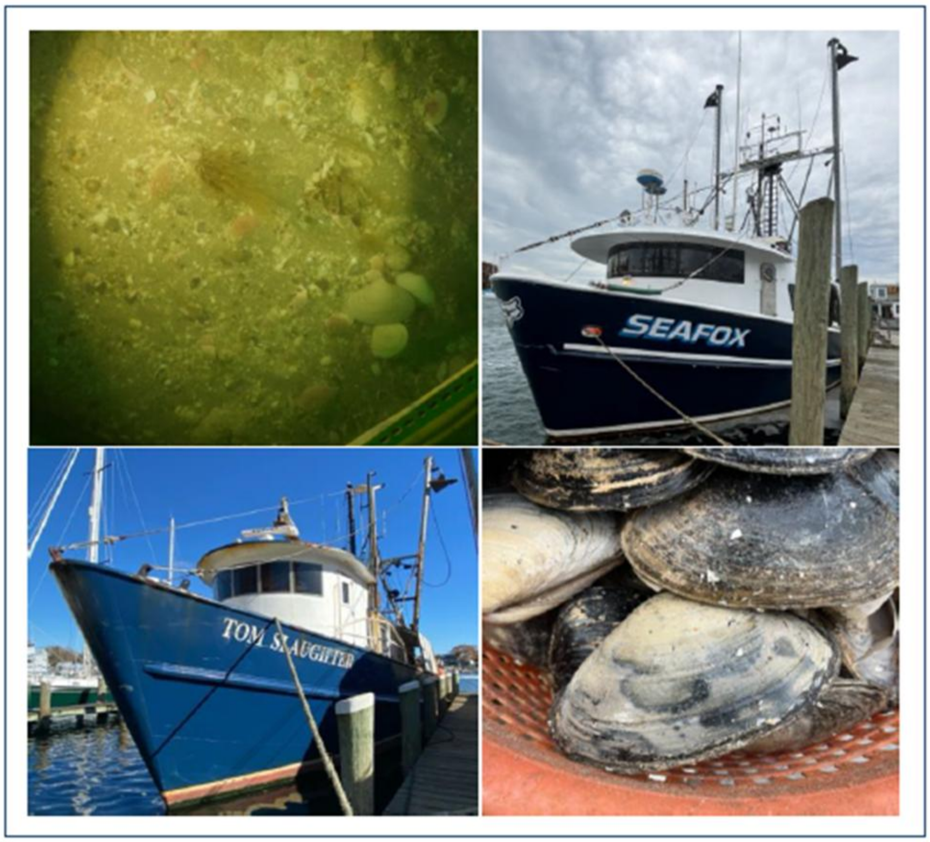

Submitted by

Natalie Jennings, Luisa Garcia, Farrell Davis, and Ryan Munnelly

Coonamessett Farm Foundation, Inc.

EXECUTIVE SUMMARY

This report presents the methods, results, and discussion of work conducted under EFP 23073, a cooperative research project by Coonamessett Farm Foundation in partnership with the commercial surfclam industry to investigate benthic habitats within the Davis Bank East (DBE) research area of the Great South Channel Habitat Management Area. Building upon EFP 19066, the project combined repeated multibeam sonar surveys, drop-camera imagery, and commercial fishing observations, relationships between acoustic backscatter and seafloor characteristics, and the effects of hydraulic surfclam dredging in a high-energy continental shelf environment. The project objectives were to characterize benthic habitats, evaluate multibeam backscatter as a habitat mapping tool, assess habitat change associated with hydraulic surfclam dredging, and demonstrate the effectiveness of cooperative research for long-term habitat monitoring.

Compensation fishing trips began in DBE in August 2024 before relocating to Rose and Crown (RC) research area because catch rates in DBE were insufficient to support continued fishing. Compensation fishing occurred there until the end of June 2026. Catch-per-unit-effort was comparatively lower in DBE (11,004.31 versus 18,236.46 bushels km^2 in RC) and trips consisted of longer tows and greater swept area per bushel landed. In total, 8.75 km^2 of seafloor was swept for approximately 107,000 bushels landed (an estimated \$3.2 million in ex-vessel value). Landings supported the research surveys of the DBE study site.

Repeated seasonal habitat surveys demonstrated that DBE is a heterogeneous seafloor composed primarily of sand, shell hash, and localized hard-bottom habitat. Dense hydrozoans aggregations, blue mussel beds or clumps, and sensitive habitat features like corals, and sea pens were not observed within DBE. Continuous multibeam surveys document substantial natural habitat dynamics, with an estimated 10.3-14.2 million m^3 of net sediment redistribution occurring between successive surveys. Individual sand waves migrated 13.5 and 20.7 m to the southwest between north polygon surveys and changed in length, width, and height from the seafloor. Widespread changes in backscatter occurred across the survey area between surveys.

Multibeam backscatter proved to be a reliable indicator of substrate composition. Mean backscatter was consistently related to total rock abundance, with survey models explaining 21-32% of the variation in backscatter. Relationships between backscatter and epifaunal communities were weak, suggesting that multibeam mapping effectively characterized physical habitat but should be complemented by optical ground-truth mechanisms to evaluate cm-level biological communities.

Analysis of fishing exposure indicated that natural sediment redistribution was the dominant drive of substrate change. However, localized biological responses were detected, with drop-camera stations closer to observed fishing tows exhibiting greater declines in bryozoan cover ($\rho = -0.35$, adjusted $p = 0.004$). Distance to observed tow tracks explained approximately 17% of epifaunal variation but only 3% of substrate variation, indicating that sessile epifaunal communities may be more sensitive indicators of localized fishing disturbance than substrate composition alone.

Overall, this project demonstrates that repeated acoustic mapping combined with optical surveys provides an effective framework for distinguishing natural habitat variability from localized fishing effects in high-energy continental shelf environments. Compensation fishing provided access to the surfclam resource while supporting repeated habitat surveys, scientific observations, and long-term monitoring, demonstrating the value of cooperative research partnerships for advancing habitat research and informing fisheries management. The results improve understanding of habitat processes on Nantucket Shoals, validate multibeam backscatter as a tool for broad-scale habitat characterization, identify epifaunal communities as sensitive indicators of localized fishing disturbance, and provide a scientific foundation for future monitoring and management within the Great South Channel Habitat Management Area.

Table of Contents

List of Figures

List of Tables

1. Introduction

Marine benthic habitat mapping provides a framework for understanding the physical and biological processes that structure seafloor ecosystems and has become an important tool for the conservation and management of marine resources. By integrating information from biology, ecology, geology, hydrography, oceanography, and geophysics, habitat mapping characterizes the distribution and spatial organization of benthic habitats (Diaz *et al*., 2004; Brown *et al*., 2011). Advances in acoustic remote sensing now enable continuous, high-resolution measurements of bathymetry and backscatter over broad spatial scales, providing an efficient means of characterizing seafloor morphology and substrate variability (Kenny *et al*., 2003). These approaches are typically derived from observations collected over a discrete period and are treated as static observations, however, many continental shelf environments are continually reshaped by physical processes that alter habitat characteristics over seasonal and interannual time scales (Brown *et al*. 2011; Uchupi, 1968; Harris *et al*., 2012).

Nantucket Shoals is a region of depositional seabed features formed by the Laurentide Ice sheet recession, resulting in a complex dune-like topography of sand ridges, troughs, and sand-wave fields (Uchupi, 1968). Unconsolidated sediments consist of reworked glacial deposits and depths range from one to 50 m (Ziegler *et al*., 1964). Tidal currents frequently above 0.6-1.0 ms^{-1} (Greenberg, 1983) and storm events reshape sandy areas, creating north-south channels between ridges and driving net sediment transport to the south and southwest (Uchupi, 1968; Limeburner and Beardsley, 1982; Twitchell, 1983). This dynamic environment is maintained by high bottom shear stress, which frequently exceeds the threshold required to mobilize sediments ranging from sand to cobbles, producing a patchwork of more stable gravel outcrops interspersed with large mobile sand deposits that can shift on biweekly timescales (Wentworth, 1922; Soulsby, 1997; Harris *et al*., 2012).

In addition to its complex geomorphology, Nantucket Shoals is strongly influenced by oceanographic processes including tidal mixing and advection from adjacent water masses. Cooler water from the Gulf of Maine and warmer waters from Nantucket Sound seasonally shape the water column (Limeburner and Beardsley, 1982). Water warms as it moves across the shoals during spring and summer and cools during winter, resulting in seasonal stratification from June through September and a well-mixed water column during winter. Sea surface temperatures range from approximately 0-3°C in late winter to 20-22°C in late summer (Fewings and Lentz, 2011). Despite these seasonal variations, the shoals generally remain cooler than surrounding waters due to persistent tidal currents and localized wind-driven mixing (Limeburner and Beardsley, 1982).

Together, the geomorphic and oceanographic processes produce a heterogeneous seafloor. Fine sand, shell hash, gravel, cobbles, and localized boulders occur in close proximity, creating abrupt changes in substrate composition over short spatial scales that change over time (Uchupi, 1968). Variation in substrate grain size, stability, and structural complexity influences benthic communities by providing different settlement surfaces for sessile epifauna, refuge for mobile invertebrates, and habitat for commercially and ecologically important species (Auster *et al*., 1995; Kostylev *et al*., 2001; Brown *et al*., 2011). Characterizing the spatial distribution and temporal variability of these habitat patches is therefore fundamental to understanding habitat function and evaluating the effects of natural and anthropogenic disturbance.

Because of the habitat diversity and its ecological importance, portions of Nantucket Shoals have received federal habitat protection. The 2,566 km^2 Great South Channel Habitat Management Area (GSC HMA) was closed in 2018 to protect perceived vulnerable benthic habitats and associated federally managed species, such as Atlantic cod (*Gadus morhua*). Research needs for the GSC HMA were finalized by the New England Fishery Management Council (Council) in 2019 and exemption areas were designated for research projects operating under Exempted Fishing Permits (EFP). Despite its protected status, relatively little contemporary information exists on fine-scale habitat variability and temporal change within the GSC HMA, particularly in areas that historically supported commercial surfclam resources.

This study was conducted under EFP 23073 and builds upon research conducted from 2020-2022 under EFP 19066. The previous results documented a fine-scale mosaic of sand, shell hash, gravel, cobbles, and boulders within a 24 km^2 study area and demonstrated that substrate composition varied seasonally over tens of meters. Dense blue mussel beds and mussel clumps were characteristic in the study area, along with colonial stalked-hydrozoan aggregations and hard surfaces encrusted with barnacles and low-relief bryozoan. The study also identified positive relationships between surfclam catch and intermediate-sized coarse substrates, suggesting that habitat heterogeneity may influence surfclam distribution (Jennings *et al*., 2022). These findings demonstrated substantial spatial and seasonal variability in benthic habitats, but they relied on labor-intensive seafloor video annotation that limited the scalability of efficient habitat characterization. Consequently, it remained unclear whether acoustic habitat metrics could provide a reliable surrogate for repeated habitat assessment relevant to biological communities.

The dynamic physical environment of the shoals creates both persistent disturbance and variable thermal regimes, with implications for benthic habitats and species composition (Sousa, 1984). Among the species influenced by these conditions, the Atlantic surfclam (*Spisula solidissima*) is particularly relevant in this area. Surfclams are large and long-lived, siphon- feeding bivalves that live infaunally (Jones *et al*., 1978). Surfclams support a productive commercial fishery and are extracted using a hydraulic fishing dredge. The geomorphology and hydrography of Nantucket Shoals create favorable foraging conditions by concentrating prey through tidal mixing and upwelling from the Great South Channel and by the natural resuspension of organic matter from the sediments (Munroe *et al*., 2013). Surfclams have been found to grow more quickly and to a larger size there than other areas of their range (Powell *et al*., 2021).

Due to the habitat variability withing the Nantucket Shoals complex, comprehensive characterization requires integrating observations collected at multiple spatial and temporal scales. Multibeam sonar provides a rapid means to produce continuous bathymetric and backscatter charts that can be related to substrate composition identified from imagery at discrete drop-camera sites. Together, these datasets link acoustic patterns to observed habitat characteristics, allowing habitat heterogeneity to be quantified across the study area and evaluated through repeated seasonal surveys. Collecting the data aboard commercial surfclam vessels, in partnership with vessel owners, captains, and crew, provided an efficient and cost-effective sampling platform. This study uses the paired approach to determine whether backscatter reliably tracks substrate and rock characteristics observed in drop-camera imagery, and to assess whether habitat change can be attributed to natural and anthropogenic factors.

2. Project Goal and Objectives

The primary goal of this research is to identify benthic habitats and species associations present in the study area of the GSC HMA and gauge their vulnerability to fishing to fill an urgent data gap and inform management decisions.

The specific objectives of this study are:

1. Map benthic features within the Davis Bank East fishery exemption area using multibeam sonar
2. Assess temporal variability in substrate composition using repeated multibeam surveys supported by drop-camera survey ground-truthing
3. Characterize benthic communities associated with different habitat types using drop-camera imagery
4. Evaluate the effectiveness of compensation fishing as a cooperative research framework that uses commercial fishing vessels as research platforms and compensation fishing landings to support long-term habitat monitoring

3. Methods

3.1 Study Area

Within the GSC HMA, there are three designated areas set aside for the surfclam fishermen to commercially fish and two areas set aside for research, the Rose and Crown (RC) and Davis Bank East (DBE). The original study design called for an initial baseline survey of the entire DBE study area, followed by one year of compensation fishing in the southern polygon while repeated seasonal habitat surveys were conducted in the northern polygon. A second survey of the study area was then planned to evaluate temporal shifts in substate composition (**Figure 1a**). However, once compensation fishing trips began, the captains and crew encountered difficulty landing surfclams at commercially efficient rates of >1 surfclam cage per hour in the south polygon.

The survey area was then split along an east-west boundary with compensation fishing occurring in the east and surveys in the west (**Figure 1b**). Despite the change, fishing efficiency remained too low to support research costs. Compensation fishing efforts subsequently moved to a 69 km^2 area in RC (**Figure 1b**); which overlapped the area fished under EFP 19066. Survey efforts remained in DBE. Catch rate data from both areas, including the differences that ultimately drove this shift in effort, are presented in Section 4.4.

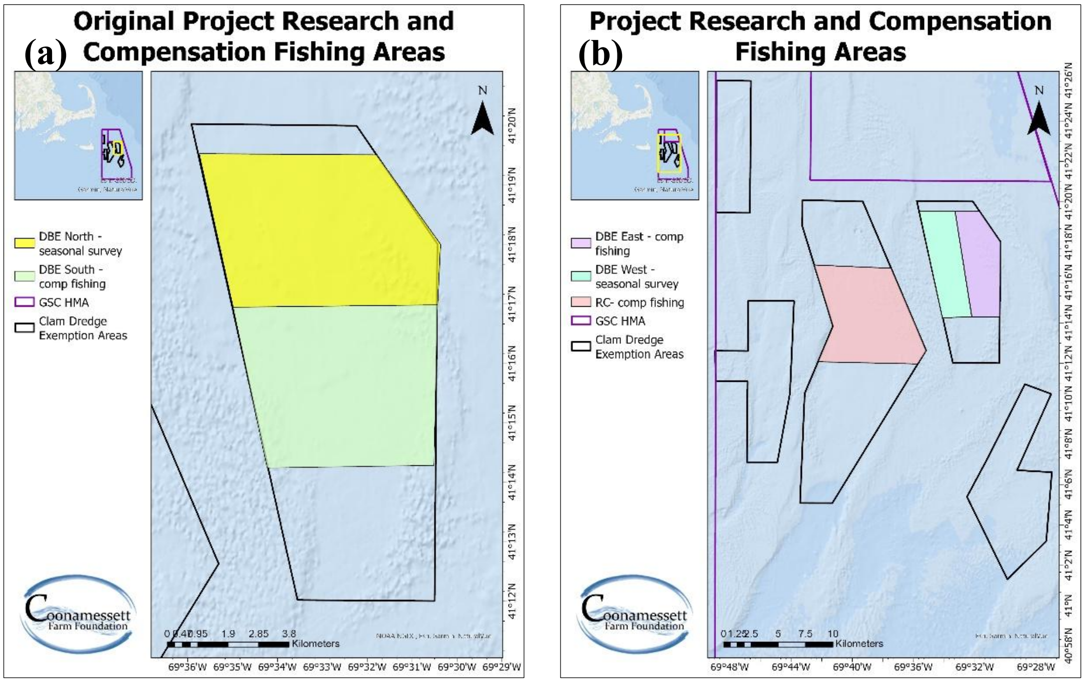

Figure 1. Davis Bank research area within the Great South Channel Habitat Management Area. (a) Original project design with proposed northern and southern survey polygons. (b) Final project configuration following revision of the compensation fishing areas. Repeated surveys were conducted within the north survey area to capture fished and unfished areas(a).

3.2 Data Collection

Data was collected at sea on dedicated research surveys or compensation fishing trips accomplished aboard the FVs *Seafox*, *Tom Slaughter*, and *Tom Slaughter III*. Survey trips consisted of multibeam sonar and drop-camera surveys and were done in a paired fashion, where drop-camera was completed following a multibeam survey to ground-truth sediment and epifaunal composition. Data were organized and quality-controlled within a relational database before use in analyses.

3.2.1 Sonar surveys

Multibeam data were collected using a 160 kHz hull-mounted Furuno F3 WASSP multibeam system with integrated real-time-kinematics positioning and inertial measurement units on the FV *Tom Slaughter*. Survey transect lines were oriented east-west and spaced 40 m apart equally to provide 25-50% overlap between adjacent transect lines due to the system's 1:3 depth:swath ratio of the beam pattern. Surveys were conducted between 6-8 knots. Multibeam surveys were completed over 21 total survey days on the FV *Tom Slaughter* in August 2024 for the south polygon, and August 2024, May 2025, and June 2026 for the north polygon.

3.2.2 Drop-camera surveys

Drop-camera surveys were completed over 9 total survey days on the FV *Seafox* in August 2024 for the south polygon, and September 2024, May 2025, and June 2026 for the north polygon. Station selection was random-stratified based on bathymetry and backscatter from the first multibeam survey. Mean distance between fixed stations was 0.42 km. The drop-camera array was outfitted with a down-facing time lapse camera (Marine Acoustic Technologies, Inc., Falmouth, MA) recording 1 image every 5 s^{-1} with synchronized strobe lighting, a downward-facing high-definition video camera, and a horizontal facing video camera (GoPro Hero+). The camera array was deployed at each station and held in place on the seafloor for a minimum of 15 s. A temperature and depth logger (Lotek, Inc., Ontario, Canada) was attached to the frame to collect station-specific temperature data. Images were recorded at a height of 0.95 m above the seafloor.

3.2.3 Compensation fishing trips

For 25% of the fishing trips allotted under the EFP, a CFF scientist was onboard collecting tow and catch composition data. Information collected by tow included start and end GPS coordinates and times, depth, vessel speed, tidal stage, and number of bushels caught. A one-bushel subsample was taken per tow to assess species composition, abundance, and weights. Weights were collected with a Marel M1100 PL3260 motion compensated scale. Surfclams were measured by a fixed-interval measuring board in 5 mm bins.

3.3 Image Analysis

3.3.1 Multibeam bathymetry and backscatter

Multibeam sonar data collected during each survey were processed using SonarWiz 8.7 (Chesapeake Technology, Mountain View, CA) software. Beam segments were cropped to reduce error at the outer beam areas and patch test corrections were applied to account for pitch and roll. Tide files were created from the Great Point tide station on Nantucket, MA (NOAA station 8448566), and a 45-minute advanced offset was applied based on the known difference between this tide station and the DBE survey area. Bathymetry and backscatter grids were generated with 10 cm spatial precision and gaps in the survey ≤ 25 m were filled using inverse-distance weighted interpolation. Acoustic data was processed and corrected for tides across all surveys and sound velocity measurements of 1488-1498 m/s in August of 2024 when the area experiences well documented water column stratification.

Final bathymetry and backscatter files were exported as GeoTIFs with 25 cm spatial resolution and visualized in ArcGIS Pro (Esri, Redlands, CA) for spatial analyses and figure production. Acoustic data collected in August of 2024 was corrected with sound velocity measurements collected with a Valeport miniSVP (Teledyne Valeport, Totnes, U.K.) due to water column stratification that characterizes the area during the summer months (Limeburner and Beardsley, 1982). Sound velocity profiles were not collected during the May 2025 and June 2026 surveys because the water column is typically well mixed outside the summer stratification period.

To evaluate physical changes in bedform morphology independent of raster-based bathymetric comparisons explained in Section 3.5, ten individual sand waves within the north polygon were compared across the three repeat surveys. Each sand wave was measured by length, width, and height, and the distance and angle moved by the leading edge of the sand waves. Distance moved was divided by time elapsed to calculate the approximate daily movement rate.

3.3.2 Drop-camera still imagery

Still images were analyzed in the PhotoQuad software (Trygonis and Sini, 2012), which allows for image calibration using a known reference distance and the use of a user-defined species library (see **Table A1** in Appendix A for the full library list). Two calibration bars of known lengths (1 and 2.3 cm) on the camera stand frame and were visible in all images. The camera height above the seafloor (0.95 m) and field of view remained constant throughout the surveys. A single image was selected and annotated per station to standardize effort across sites. Images that were blurry, had suspended sediment, or did not have clear bottom contact were not excluded. Because images within a station were taken only seconds apart and represented nearly identical bottom footprints, additional images from the same station were not treated as independent replicates.

A 100-point grid was generated within the calibrated image area (the quadrat) for each annotated image, and annotation occurred only within this bounded region. Where a point intersected a rock, shell fragment, or epifaunal organism, the corresponding feature was outlined as a region of interest and classified using the species library (**Table A1**), which included substrate categories (e.g., sand, sand with shell hash, rock), shell material (clam, mussel, other), and epifaunal taxa (barnacles, encrusting bryozoans, hydrozoans). Where multiple epifaunal taxa co-occurred within a region of interest, only the most visually dominant taxon was recorded; as a result, percent-cover estimates for dominant taxa may slightly overrepresent true monospecific coverage in areas of overlapping epifaunal growth. In total, 399 images were manually annotated across all four surveys (the first drop-camera survey in the south box had 99 stations). All images were annotated by two experienced annotators.

In this report, the term "rock" refers to a hard sediment particle of any size. Particle size class was assigned after measurement using the maximum axis length following the approximate Wentworth (1922) diameter classification (**Table 1**). Because maximum axis length was used rather than measured axis, this method may overestimate some particles sizes, but it will not underestimate it.

Table 1. Rock particles measured in the Davis Bank East survey area included particles ranging from granule to boulder.

Substrate Particle	Wentworth Scale (cm)
Granule	0.2 to < 0.4
Pebble	0.4 to <6.4
Cobble	6.4 to < 25.6
Boulder	25.6 to <409.6

3.4 Backscatter Extraction and Habitat Metric Compilation

Coordinates from the repeated north polygon surveys were compared among all survey pairs to quantify station re-sampling accuracy. Pairwise distances between repeated drops were calculated and the resulting distribution of re-sampling distances was used to identify a representative spatial scale for extracting multibeam backscatter. Circular buffers of 50, 65, 100, 150, 200 m were selected to represent increasing levels of realized station-placement variability while maintaining a spatial scale relevant to the habitat observed by the camera.

Multibeam backscatter rasters were imported into ArcGIS Pro and zonal statistics were calculated for each station buffer (Collier and Brown, 2005). Values from each survey and buffer distance were compiled into a primary backscatter dataset.

Image-derived habitat metrics were summarized at the station level and merged with corresponding backscatter statistics using survey and station identifiers, and buffer distances. Habitat variables included rock abundance and particle size, substrate composition (sand, shell hash, and identifiable shell fragments), and epifaunal cover (barnacles, hydrozoan, and encrusting bryozoan). See **Appendix Table A3** for a complete list of habitat metrics by station.

3.5 Statistical Analyses

Data management and statistical analyses were conducted in R (R Core Team, 2025).

3.5.1 Fishing effects analyses

Ninety paired drop-camera stations were surveyed twice with drop-camera over an area that experienced a range of dredge fishing exposure. Fishing exposure was quantified as Swept Area Ratio (SAR) extracted from tow coordinates during CFF-observed trips. SAR is a standardized index and defined as the cumulative seafloor area contacted by fishing gear divided by the total area of the grid cell over a given period (Eigaard *et al*., 2016, 2017). For this analysis, SAR values were rasterized at a 10-meter grid resolution and averaged within an 84 m buffer around each station.

Station-level SAR reflected only CFF-observed tows, which was 25% of total fishing effort in DBE, and likely underestimates the true exposure at many drop-camera stations. The primary exposure metric used in the cross-sectional substrate and epifauna analyses below is therefore the distance from each drop-camera station to the nearest observed tow track, computed using the 177 recorded tows located within the multibeam-survey footprint. For the longitudinal (persistence over time) and Time Point diagnostic analyses reported later, stations were additionally classified as "Fished" (SAR sum > 0) or "Unfished" (SAR sum = 0) as a secondary, time-invariant exposure label; 17 of 99 stations were classified as Fished under this definition.

Change between surveys (Δ = August 2024 – May 2025) was calculated for each station across substrate/grain-size variables (mean and maximum rock size, fine and coarse rock counts, sand, sand-dune, and shell point counts) and epifauna cover variables (hydrozoan and bryozoan cover). Univariate comparisons used Spearman correlations between distance-to-nearest-tow and each of the 13 delta variables, with Benjamini-Hochberg correction applied across all variables tested. Because several substrate variables were correlated with one another, a multivariate approach, PERMANOVA, was used to test whether distance-to-tow explains joint substrate/grain-size change and, separately, joint epifauna cover change, without the power penalty of per-variable correction. Before treating any distance-based result as confirmed, a robustness check recalculated each significant correlation after sequentially removing the stations closest to and farthest from a tow track, to test whether a result depended on either extreme of the distance distribution rather than reflecting a genuine gradient.

An additional analysis assessed if dredge disturbance was detectable with multi-beam sonar. To do this, sample points were generated at 10 m intervals along dredge tow paths (n = 21,678) that occurred in the east half of the polygon and randomly placed greater than 25 m away from them (n = 2,404). The Δbackscatter (dB) data was then extracted from the raster at these locations.

3.5.2 Backscatter-habitat relationships

Extracted backscatter metrics were compared with habitat metrics derived from drop-camera imagery across all stations and surveys. Linear regression analyses were used to quantify relationships, while Kruskal-Wallis tests were used to evaluate differences in mean backscatter among dominant substrate classes. Analyses focused on identifying habitat characteristics most strongly associated with backscatter and evaluating whether backscatter primarily reflected substrate composition, rock abundance, or epifaunal cover.

4. Results

4.1 Habitat Characterization

Multibeam and drop-camera research surveys were completed of the north and south polygons in August and September 2024. Repeated surveys of the north polygon were completed in May 2025 and June 2026.

Seafloor mosaics were generated for the four surveys to characterize bathymetry within the study area (**Figure 2**). The surveys revealed a heterogeneous seabed composed of broad sand waves, depressions, and localized areas of elevated relief (5-58 m depth). These large-scale geomorphic features were generally consistent among repeated surveys, providing the physical framework for subsequent habitat analyses. Differences in the morphology and position of some sand-wave features were evident among surveys.

Variability in backscatter intensity indicated areas with discrete properties (**Figure 3**), which were influenced by factors such as substrate composition. Distinct areas of relatively high and low backscatter were evident throughout the study area. Areas of relatively low acoustic reflectivity consistently corresponded with the sand-wave features identified in the bathymetric mosaics, while higher reflectivity was associated with the surrounding inter-dune areas.

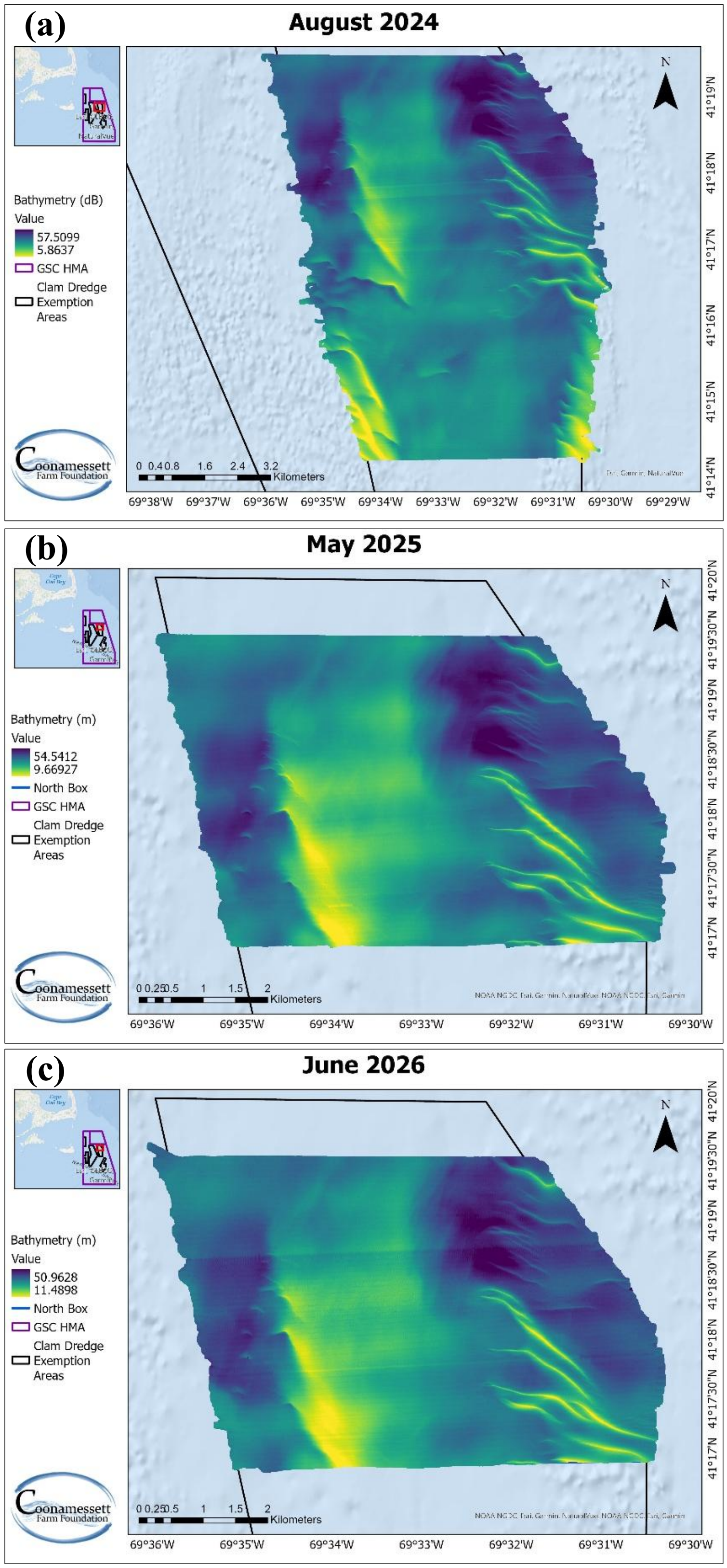

Figure 2. Bathymetry of the Davis Bank East study area measured during (a) the baseline August 2024 and repeat surveys of the north polygon in (b) May 2025, and (c) June 2026. Color scale represents depth in meters.

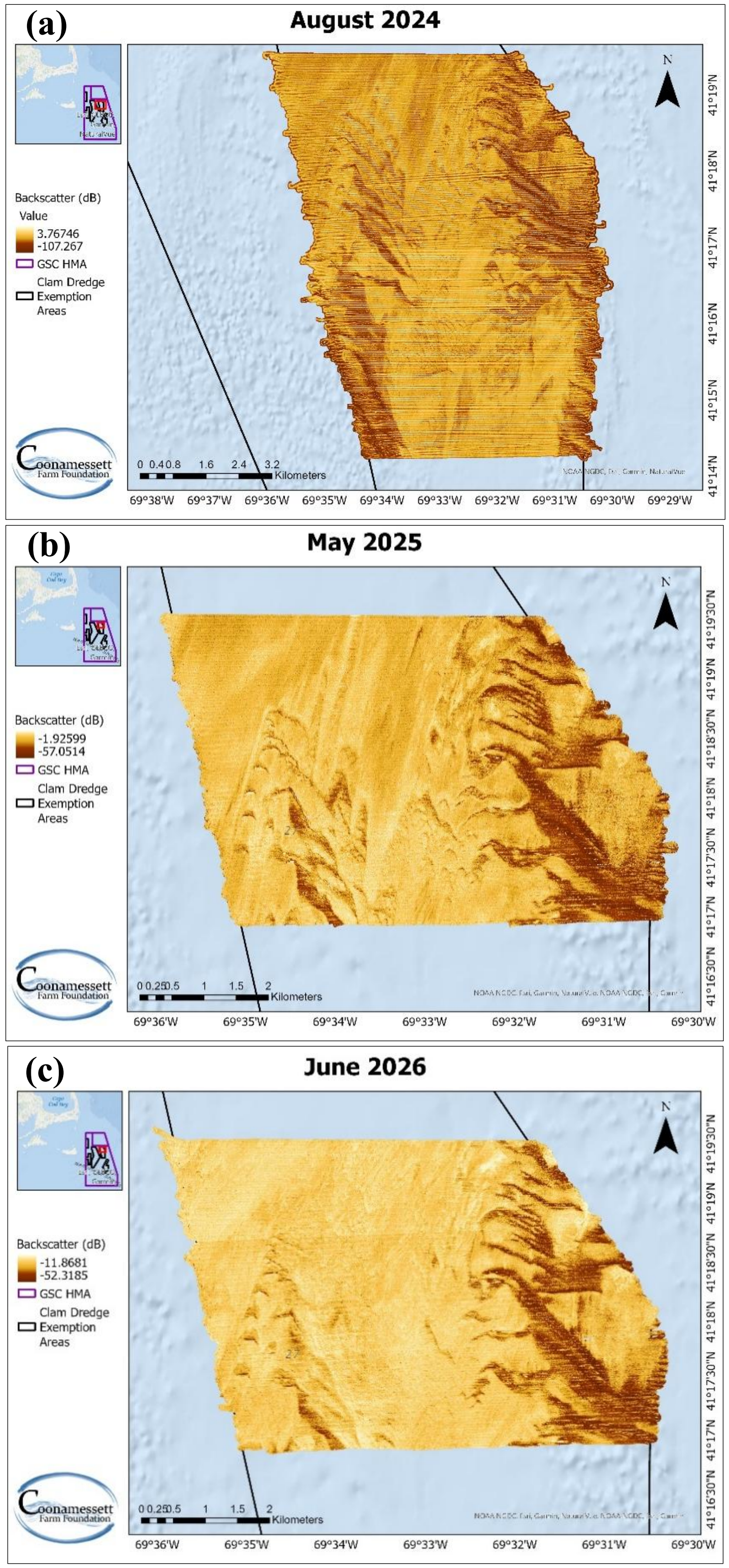

Figure 3. Backscatter of the Davis Bank East study area measured during (a) the baseline August 2024, and the repeat surveys of the north polygon in (b) May 2025, and (c) May 2026. Lighter colors represent higher backscatter intensity and darker colors represent lower backscatter intensity.

Points per drop-camera station image yielded approximately 39,800 discrete data points and were used to characterize substrate and epifaunal presence in the sample area (see **Table A2** in **Appendix A** for total point breakdown by annotated characteristic). Dominant substrate by stations and survey were measured with the 100 points-per-image annotations and determined to be sand, shell hash, and rock (**Figure 4**). Point counts for each substrate category across all surveys were 17532, 10745 and 9799, respectively.

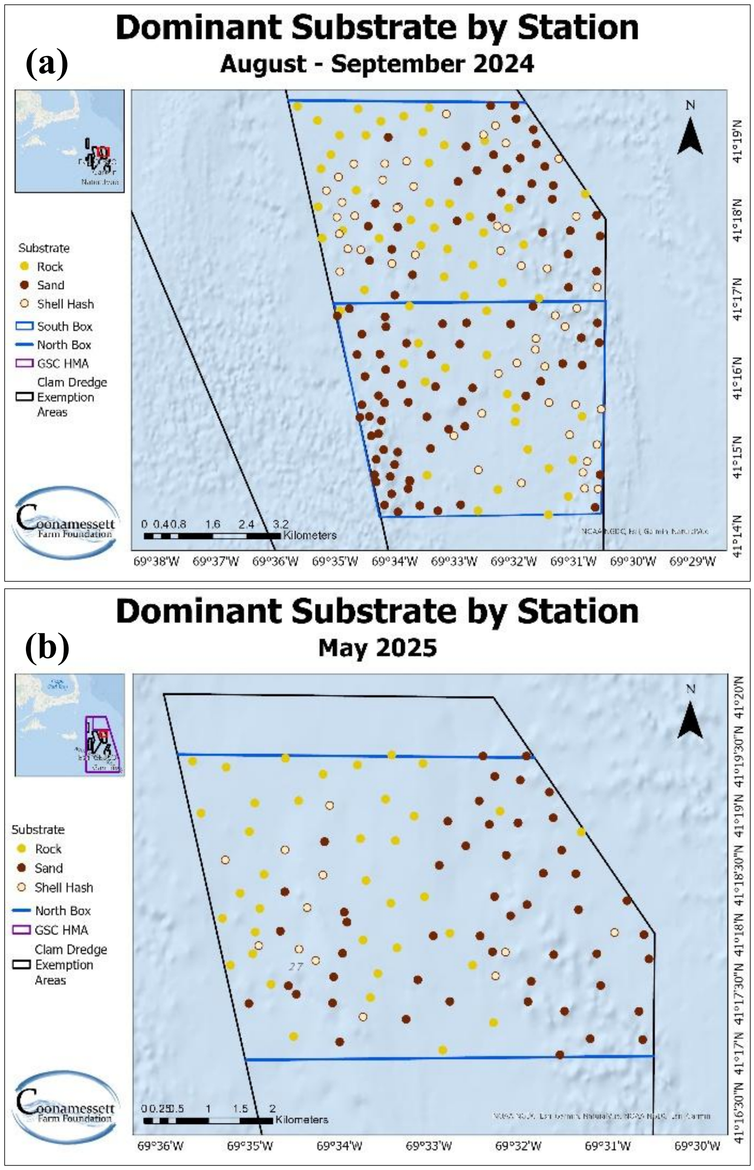

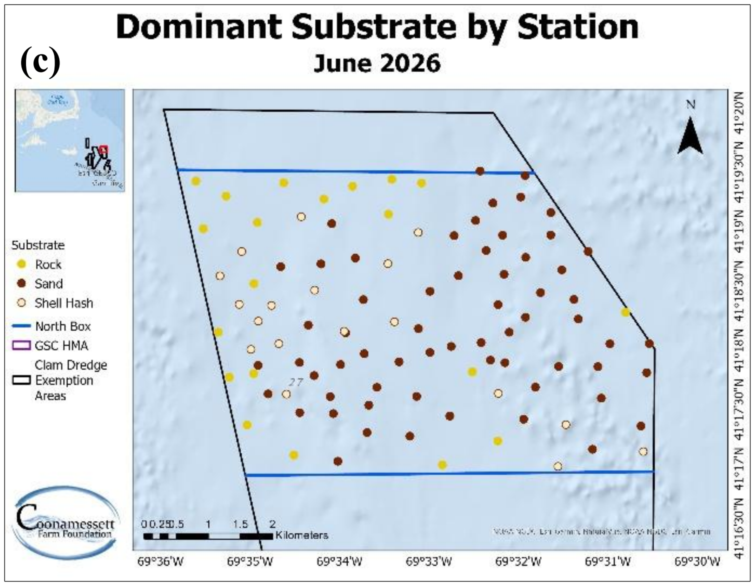

Figure 4. Dominant substrate class (sand, shell hash, or rock) at each of 100 stations per survey during (a) baseline August and September 2024 survey and repeat north polygon surveys in (b) May 2025, and (c) June 2026 in the Davis Bank East study area.

Out of 9,780 total rock particles measured, 98.4% were classified as pebbles (**Table 2**) using the maximum axis length measured in PhotoQuad. A singular boulder was observed in annotations (**Figure A1a**).

Table 2. Rock particle classification and counts measured across four surveys of the Davis Bank East study area north and south polygons.

	Rock Particle			
Drop-Camera Survey	**Granule**	**Pebble**	**Cobble**	**Boulder**
South_Aug2024	11	1844	20	0
North_Sept2024	24	3008	33	1
North_May2025	23	2818	23	0
North_June2026	9	1822	11	0

Three taxa of epifauna were documented including barnacles, stalked hydrozoans, and encrusting bryozoan. Epifauna were found growing on rocks, shells, live mussels (**Figure A1b**), and in the case of the stalked hydrozoan, coming through sandy sediment. Barnacles were the most annotated epifaunal taxa across all surveys (**Table A2**). Epifauna point totals were compared by percent stations occupied by taxa and drop-camera survey of the north polygon (**Figure 5**).

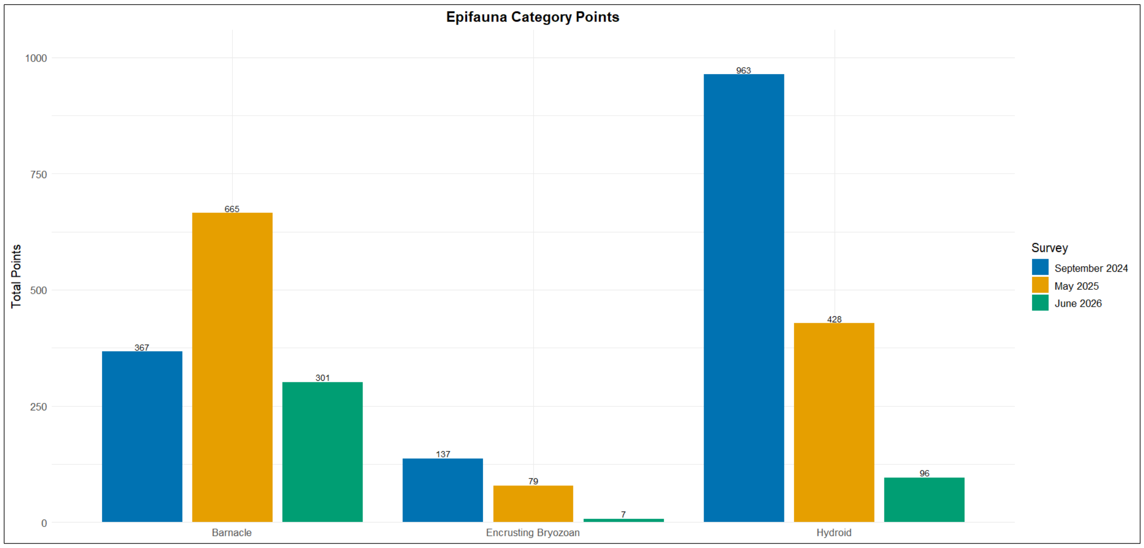

Figure 5. Total epifauna point numbers annotated from the repeat north polygon drop-camera surveys in the Davis Bank East by category.

Quasibinomial generalized linear models were used to test whether depth, station temperature, and total rock abundance improved predictions of epifaunal cover after accounting for survey differences. Depth did not improve models for barnacle or hydrozoan cover but was positively associated with bryozoan cover ($F = 7.07$, $p = 0.008$). Temperature was negatively associated with hydrozoan ($F = 5.77$, $p = 0.017$) and bryozoan cover ($F = 7.04$, $p = 0.008$), but not barnacle cover. Total rock abundance significantly improved models for all three groups and was the strongest predictor of barnacle ($F = 345.29$, $p < 0.001$), hydrozoan ($F = 243.37$, $p < 0.001$), and bryozoan cover ($F = 71.72$, $p < 0.001$).

Additional models were fitted to determine if rock characteristics influenced epifaunal cover beyond the amount of available hard substrate. Total rock abundance was the strongest predictor for all three taxa (**Table 3**). Mean and maximum rock size remained significant positive predictors after accounting for total rock abundance, whereas coarse rock (cobbles and boulders) proportion had a comparatively weaker effect and was not significant for bryozoans.

Table 3. Model statistics from epifaunal cover and rock characteristics from n = 264 stations in across four surveys in the Davis Bank East study area.

Response	**Predictor**	**Coefficient (β)**	**SE**	**F**	**p**
Barnacle	Total rock abundance	0.034	0.003	149.57	<0.001
	Mean rock size	0.667	0.065	87.76	<0.001
	Maximum rock size	0.155	0.021	44.81	<0.001
	Coarse rock proportion	3.074	1.077	4.69	0.031
Hydrozoan	Total rock abundance	0.029	0.003	95.54	<0.001
	Mean rock size	0.662	0.076	65.28	<0.001

Response	Predictor	Coefficient (β)	SE	F	p
	Maximum rock size	0.144	0.021	38.04	<0.001
	Coarse rock proportion	3.011	1.017	5.19	0.024
Bryozoan	Total rock abundance	0.021	0.005	21.1	<0.001
	Mean rock size	0.623	0.121	22.24	<0.001
	Maximum rock size	0.099	0.034	6.54	0.011
	Coarse rock proportion	1.116	2.875	0.12	0.727

Bottom temperatures measured during drop-camera deployments ranged from 7.68 to 18.37 °C across all surveys. Mean bottom temperature differed among surveys, reflecting seasonal sampling periods, with the warmest temperatures measured in September 2024 (**Figure 6**). Temperature generally decreased with increasing depth, although survey timing explained much of the observed variation.

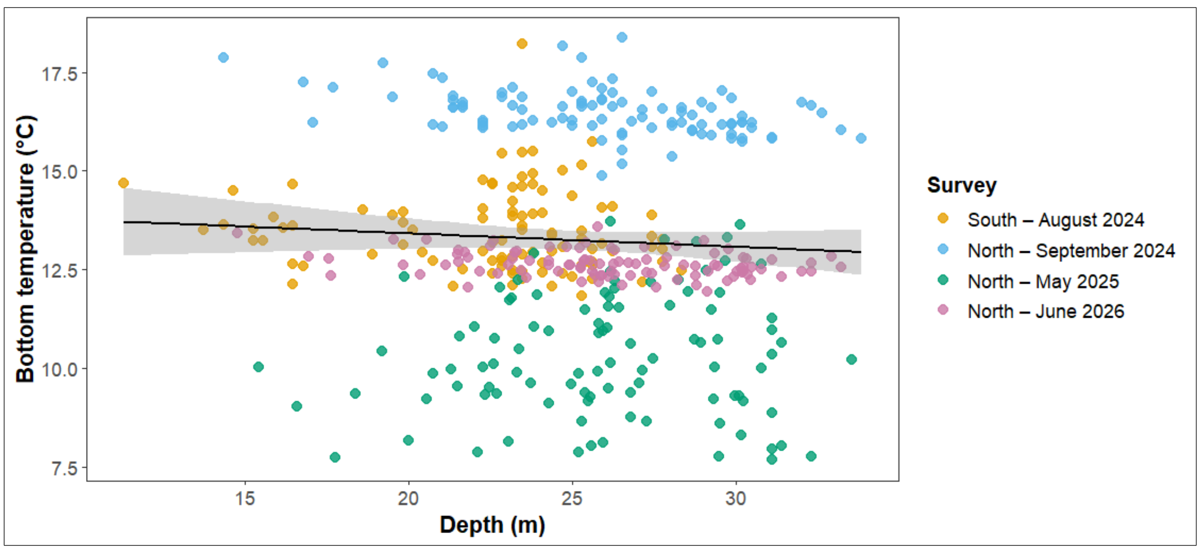

Figure 6. Bottom water temperature measured during drop-camera surveys plotted against station depth. Points are colored by survey period, and the solid line represents the overall linear regression with the 95% confidence interval (shaded).

4.2 Habitat Dynamics

4.2.1 Measured backscatter and bathymetry changes

Changes in acoustic characteristics were measured and charted between repeat surveys of the north polygon. During periods between surveys, the bathymetry and sediment composition of survey area changed substantially while the major seafloor features remained recognizable. The median change in bathymetry between August 2024 and May 2025 was -0.18 m with an overall net volume of 10,311,268 m3 estimated to have entered the system from the northeast; 12.54 km^2 increased in depth while 20.01 km^2 decreased. The median change in bathymetry between May

2025 and June 2026 surveys was -0.49 m with an overall net volume of 14,194,194 m3 of sediment entering the study area; 10.92 km^2 increased in depth while 21.25 km^2 decreased.

The median change in backscatter between August 2024 and May 2025 was -1.30 db, and 6.92 km^2 (22%) increased in backscatter while 24.98 km^2 (78%) decreased (**Figure 7a**). The median change in backscatter between May 2025 and June 2026 was 4.67 db, and 31.26 km^2 (98%) increased in backscatter, while 0.50 km^2 (2%) decreased (**Figure 7b**). The northern part of the DBE survey area showed long streaking patterns from sediment transport oriented from approximately 9 to 189°.

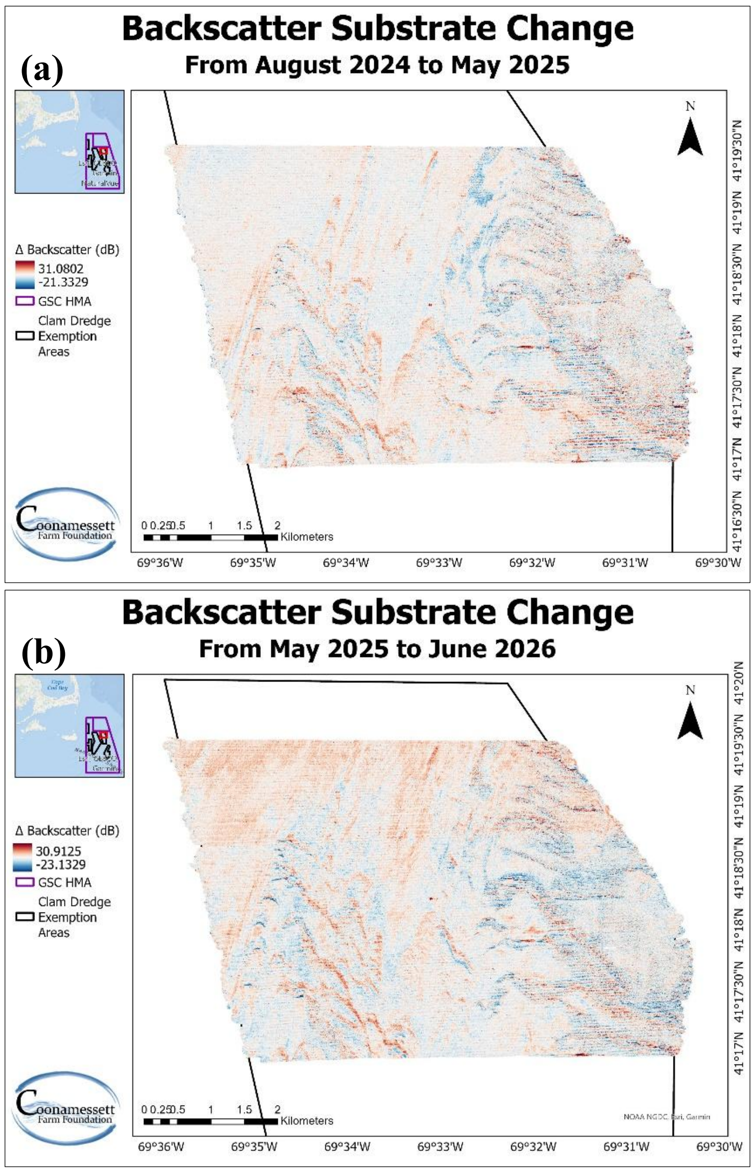

Figure 7. Changes in backscatter measured from repeat multibeam survey trips in the Davis Bank East north polygon from (a) August 2024 to May 2025 and (b) May 2025 to June 2026. Warm colors represent localized shifts to harder substrates while cool colors represent shifts to softer substrates.

The change in bathymetry can be further corroborated by the movement of individual sand waves in the survey area (**Figure 8**). Tracked sand waves ranged in size from 38 to 293 m (156 ± 84 m) in length, 8.11 to 69 m (28 ± 17 m) in maximum width, and 0.9 to 5.1 (2.9 ± 1.5 m) m in crest height. These features experienced a mean length change of -20 to 20 m (-0.9 ± 13) between August 2024 and May 2025 and -0.6 to 51.7 m (20.9 ± 17.9) between May 2025 and June 2026. Mean width changed by 11.2 to 12.4 (2.0 ± 4.0) between August 2024 and May 2025 and -16.5 to 12.4 (-1.8 ± 9.4) between May 2025 and June 2026. Mean height changed by -0.6 to 0.3 m (-0.1 ± 0.3) between August 2024 and May 2025 and -0.24 to 2 (0.9 ± 0.7) between surveys May 2025 and June 2026. These features moved 13.5 ± 8.5 m to the southwest between surveys August 2024 to May 2025, and 20.7 ± 5.1 m between surveys May 2025 to June 2026. The overall movement rate of 5.4 ± 2.7 cm per day. The mean angle of movement was 191.7 ± 8.3°.

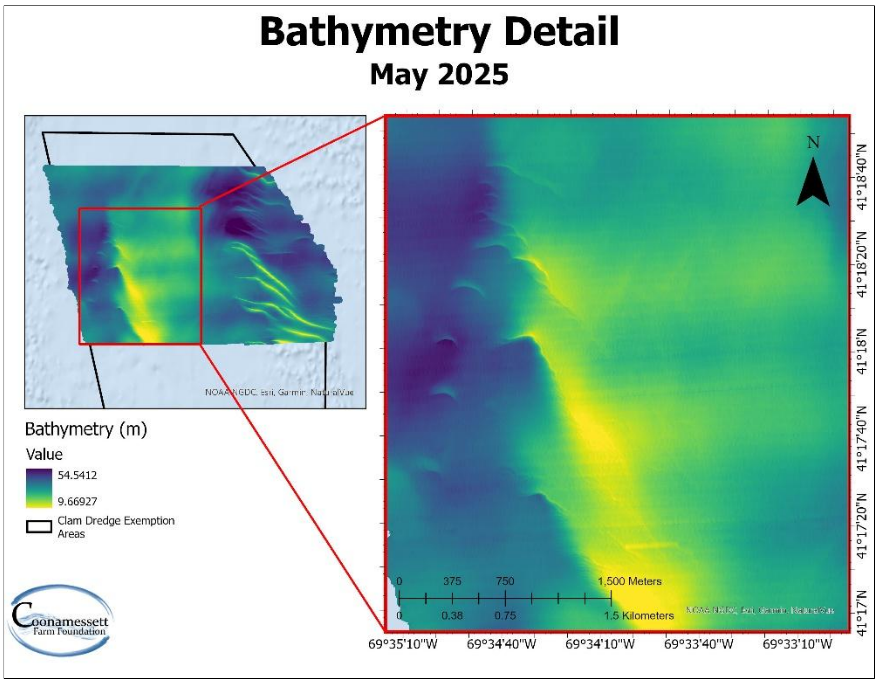

Figure 8. Bathymetrical charting of the north polygon in May 2025 showing detail of large sand dunes and sand waves.

4.2.2 North polygon fishing exposure

Among the individual habitat variables examined between the Augst 2024 and May 2025 surveys, Δ Bryozoan cover (Spearman ρ = -0.35, adjusted p = 0.004) and Δ Other Shell points (ρ = 0.34, adjusted p = 0.004) showed significant relationships with distance-to-tow (**Figure 9a**). Stations closer to a tracked tow showed more negative bryozoan cover change and more positive other shell-point change. Δ Sand points (ρ = -0.22, adjusted p = 0.064) and Δ Fine rock count (ρ = 0.23, adjusted p = 0.064) were borderline but did not clear BH correction. All other substrate and epifauna variables were not significant (adjusted p > 0.07 throughout, (**Figure 9a**).

The correlation for every variable showing a significant relationship with distance was recalculated after sequentially removing the 1, 2, 3, 5, 10, and 15 stations closest to a tow, and again after removing the same numbers of farthest stations. Δ Bryozoan cover and Δ Other Shell points relationships strengthened, rather than weakened, when the closest stations were removed (Bryozoan cover: $p = 8.2\times10^{-5}$ with the 15 closest excluded; Other Shell points: $p = 4.4\times10^{-6}$ with the 15 closest excluded) with some sensitivity to the farthest stations. Both Δ Sand points and Δ Fine rock count lost significance in both directions of removal.

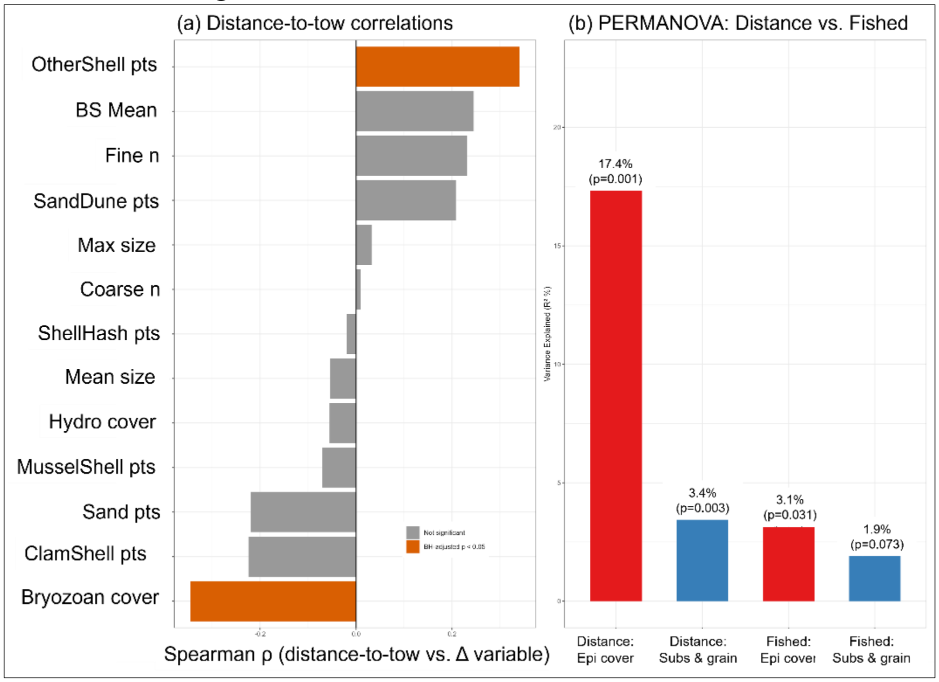

Figure 9. Relationships between fishing exposure and habitat change. (a) Spearman correlations between habitat change and distance to the nearest observed tow track. (b) Variation explained by distance to the nearest observed tow and the SAR-based fished/unfished classification in PERMANOVA models of substrate and epifaunal change.

The multivariate analysis of substrate/grain-size found that change was significantly related distance-to-tow (PERMANOVA: $F = 3.46$, $R^2 = 0.034$, $p = 0.003$). In a combined model with the station-level Fished classification, distance remained significant ($R^2 = 0.034$, $p = 0.003$), while Fished did not add further explanatory power once distance was accounted for ($R^2 = 0.019$, $p = 0.073$; **Figure 9b**).

Epifaunal community change exhibited a stronger relationship with distance-to-tow (PERMANOVA: $F = 20.37$, $R^2 = 0.174$, $p = 0.001$) with distance explaining approximately 17% of the variance, compared to no detectable relationship using the SAR-based Fished/Unfished classification alone. In the combined model, both distance ($R^2 = 0.174$, $p = 0.001$) and Fished ($R^2 = 0.031$, $p = 0.031$) remained independently significant, indicating the two captured overlapping but distinct information.

Three complementary analyses tested whether the distance-to-tow relationships detected in the cross-sectional analysis persisted between the May 2025 and June 2026 follow-ups. A linear mixed-effects model (Delta ~ Time Point * Distance-to-tow + (1|Station)) found a significant Time × Distance interaction for Δ Bryozoan cover (BH-adjusted $p < 0.001$), Δ Hydroid cover (adjusted $p = 0.020$), and Δ Clam Shell points (adjusted $p = 0.045$); while Δ Maximum rock size was borderline (adjusted $p = 0.091$). All other variables showed no significant interaction (adjusted $p > 0.13$). A direct paired comparison of interim change (June 2026 delta – May 2025 delta) against distance, among the 90 stations with both follow-ups, confirmed this for the epifauna variables specifically, Δ Hydroid cover ($\rho = -0.34$, adjusted $p = 0.012$) and Δ Bryozoan cover ($\rho = -0.31$, adjusted $p = 0.017$) both showed stations closer to an observed tow experiencing further epifauna decline between the two follow-ups, rather than remaining stable. A repeated-measures PERMANOVA confirmed this at the multivariate level for epifauna cover: Time Point ($F = 4.46$, $R^2 = 0.020$, $p = 0.001$) and distance-to-tow ($F = 31.30$, $R^2 = 0.139$, $p = 0.002$) were both significant. Critically, the Time Point:Distance interaction was significant ($F = 4.12$, $R^2 = 0.018$, $p = 0.024$) indicating the epifauna-distance relationship is not stable over time, but intensifying between the short- and long-periods between surveys.

Substrate/grain-size change showed a different pattern: Time Point ($F = 4.22$, $R^2 = 0.022$, $p = 0.001$) and distance-to-tow ($F = 5.08$, $R^2 = 0.026$, $p = 0.001$) were both significant, but the interaction was not ($F = 1.45$, $R^2 = 0.007$, $p = 0.117$). This is consistent with region-wide sediment dynamics of the Great South Channel Habitat Management Area rather than a fishing-specific effect (Jennings *et al*., 2022).

A comparative analysis of the multi-beam backscatter data revealed no significant difference between areas where fishing activity was known to have occurred between the August 2024 and May 2025 and the assumed undisturbed areas ($t = 1.6332$, $df = 2883.8$, $p = 0.1025$, **Figure 10**).

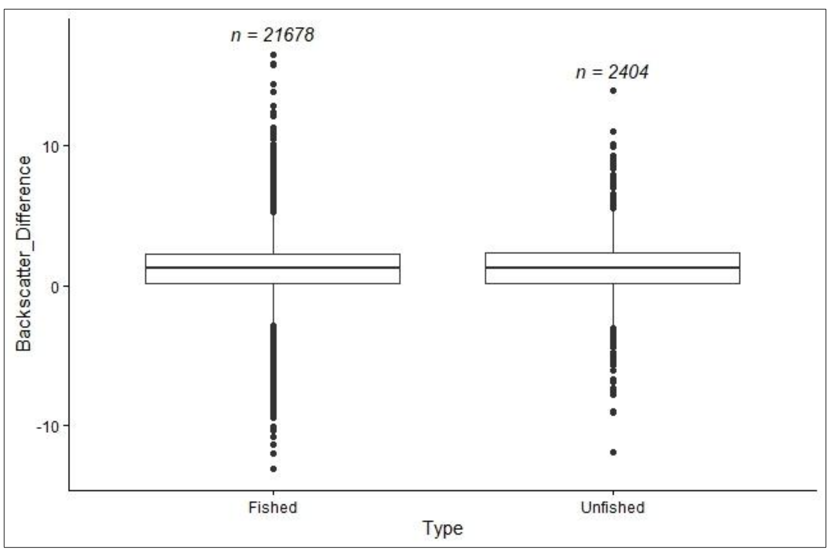

Figure 10. The Δbackscatter (dB) of the fished and unfished regions of the Davis Bank East north polygon between August 2024 and May 2025 surveys.

4.3 Backscatter Predictors of Habitat Structure

4.3.1 North polygon repeated station accuracy

Identical station waypoints were used during three repeat surveys, yielding 285 pairwise comparisons among repeated sampling of 100 stations in the north polygon. The median separation distance between repeated surveys was 64.4 m, with 90% and 95 sampling occurring within 137.9 and 160.0 m respectively (**Table 4**). Fifteen pairwise comparisons exceeded 200 m between re-samples were classified as operationally unsuccessful station occupations and excluded from backscatter analysis.

Table 4. Summary statistics describing relocation distances among repeated drop-camera station samples in the Davis Bank East north polygon (n=285 pairwise comparisons).

Metric	Value (m)
Median	64.4
Mean	73.3
Root mean square (RMS)	100.1
90^{th} percentile	137.9
95^{th} percentile	160.0
Maximum	190.5

4.3.2 Buffer optimization

Backscatter metrics were extracted at 50, 65, 100, 150, and 200 m buffer zones around the drop-camera stations. Mean backscatter differed significantly among dominant substrate classes for all surveys and buffer sizes (Kruskal-Wallis, $p < 0.001$). Relationships between backscatter and rock abundance were strongest for the 50 and 65 m buffers, whereas larger buffers (150 and 200 m) reduced model performance. Backscatter standard deviation explained up to approximately 50% of the variation in rock abundance but showed no meaningful relationship with mean rock size by station ($R^2 < 0.03$ for all models). Based on the repeat station analysis (median distance = 64.4 m) and the buffer optimization results, the 65 m extraction buffer radius was selected for subsequent habitat prediction analyses.

4.3.3 Backscatter and habitat prediction

Three dominant substrate categories were found to be sand, shell hash (sand with shell fragments), and rock. Mean backscatter differed significantly among substrate classes in all four surveys (Kruskal-Wallis, $p < 0.001$; **Figure 11**). Rock stations consistently exhibited the highest mean backscatter values, sand stations the lowest, and shell hash stations intermediate values. This pattern was consistent across surveys, indicating that backscatter effectively distinguished broad substrate types.

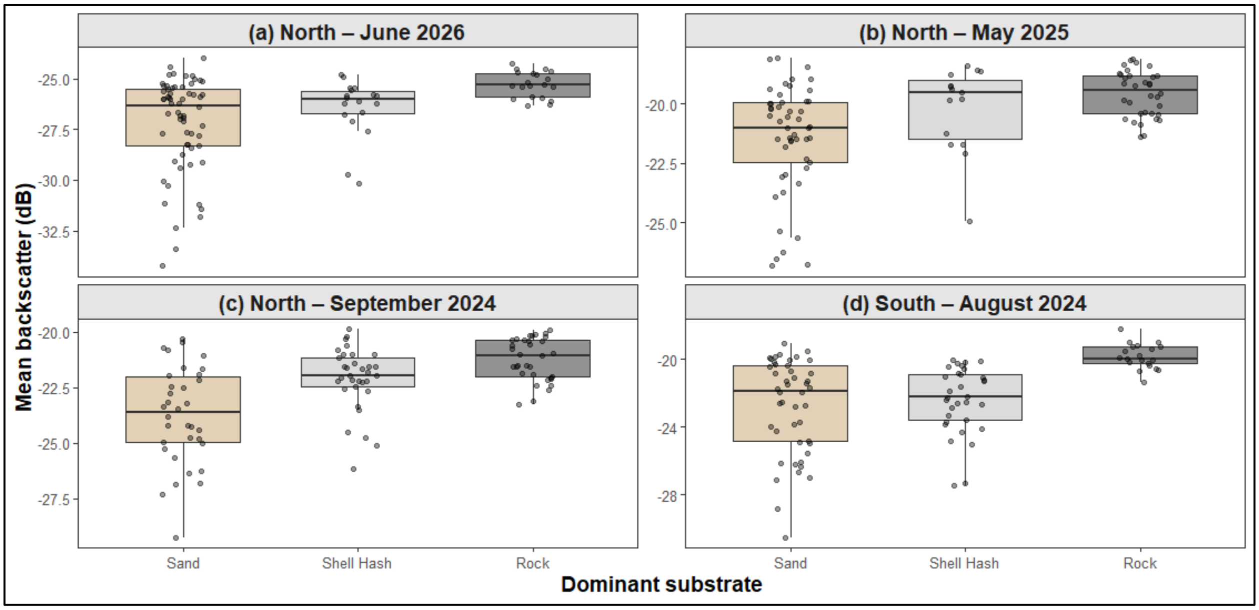

Figure 11. Dominant substrate by survey trip versus mean acoustic backscatter in the Davis Bank East survey and compensation fishing areas. Repeat surveys of the north polygon were done in (a) June 2026, (b) May 2025, and (c) September 2024. The August 2024 survey (d) was the only trip conducted in the south polygon.

Rock abundance was the strongest predictor of mean backscatter across the four surveys (R^2 = 0.21-0.32, $p < 0.001$; **Figure 12**). A multiple regression further demonstrated that both rock abundance and shell cover contributed significantly to mean backscatter, with rock abundance exhibiting was substantially stronger ($\beta = 0.048$ versus $\beta = 0.019$, adjusted $R^2 = 0.20$).

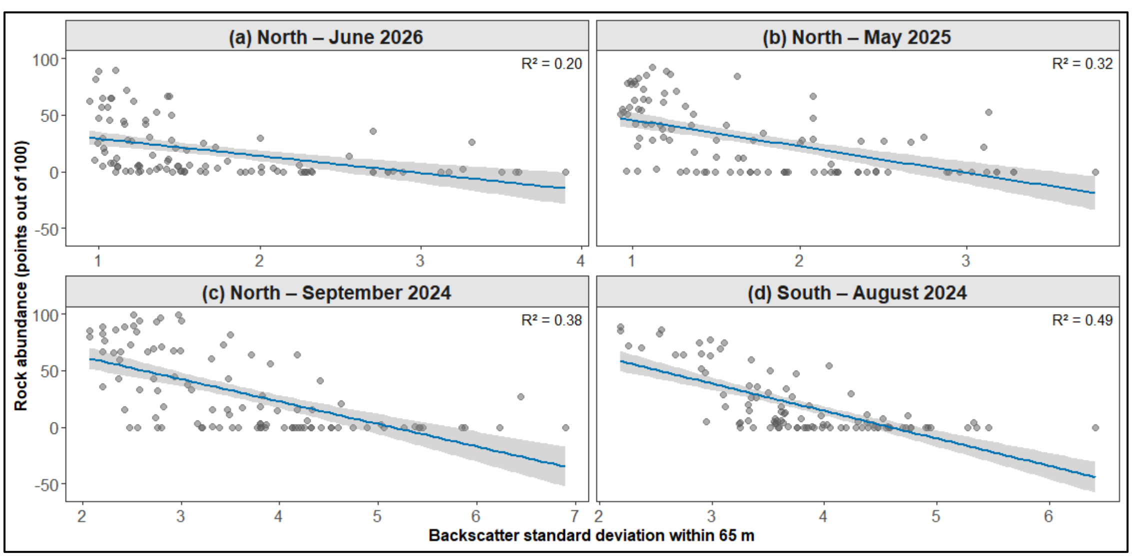

Figure 12. Linear relationships between mean backscatter (dB) and rock abundance (100-point image annotation count) for each survey conducted in Davis Bank East. Repeat surveys of the north polygon were done in (a) June 2026, (b) May 2025, and (c) September 2024. The August 2024 survey (d) was the only trip conducted in the south polygon.

Rock abundance was strongly related to backscatter, whereas rock size was a comparatively poor predictor. Mean rock size showed no meaningful relationship with backscatter, while maximum rock size exhibited only weak, survey dependent relationships ($R^2 = 0.03$-0.15). Rock size composition was further separated into fine (granules and pebbles) and coarse (cobbles and boulders) classes. Fine rock abundance was strongly associated with mean backscatter ($R^2 = 0.18$, $p < 0.001$), whereas coarse explained little variation ($R^2 = 0.02$). When both variables were included in a multiple regression analysis, only fine rock abundance remained significant, while coarse rock abundance was not ($p = 0.353$).

To evaluate whether rock abundance and rock size jointly influenced backscatter, an additive model including total rock abundance and mean rock size was examined. Mean rock size did not improve the model after accounting for total rock abundance ($F = 0.24$, $p = 0.62$). Adding an interaction between total rock abundance and mean rock size significantly improved model fit relative to the additive model ($F = 7.98$, $p = 0.005$; $\Delta AIC = 5.99$), where the positive relationship between rock abundance and mean backscatter varied with average rock size (**Figure 13**).

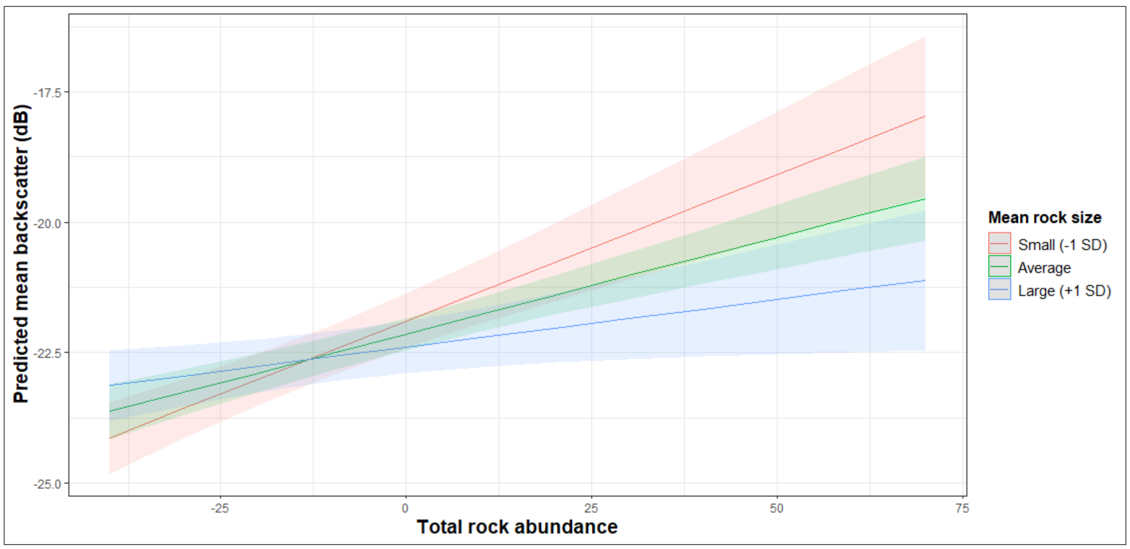

Figure 13. Predicted mean backscatter as a function of total rock abundance for stations with small (-1 SD), average, and large (+1 SD) mean rock sizes. Shaded bands represent 95% confidence intervals.

Mean backscatter decreased significantly with increasing sand cover ($R^2 = 0.17$, $p < 0.001$), although the relationship was weaker than that observed for rock abundance ($R^2 = 0.21$-$.032$). Considerable variability in mean backscatter remained among the sand-dominated stations. Many stations classified as sand-dominant also contained varying amounts of rock and shell material, suggesting that additional habitat characteristics contributed to the observed variability.

A multiple regression including shell hash, sand ripples, sand dunes, depth, and total epifauna cover explained little of the remaining variation in mean backscatter (adjusted $R^2 = 0.073$). Shell hash and depth were not significant predictors, while total epifaunal cover exhibited a weak but significant positive relationship with mean backscatter.

Relationships between mean backscatter and epifaunal cover were statistically significant in several surveys (p = 0.0158-0.0014) but consistently showed weak performance (R^2 = 0.01-0.11), indicating that backscatter was a stronger predictor of physical habitat than biological habitat (**Table 5**).

Table 5. Linear regression results evaluating mean backscatter amplitude and epifaunal metrics compared to rock abundance.

Response	R^2 Ranges	Interpretation
Rock cover	0.21-0.32	Moderate positive relationship
Total epifauna	0.04-0.10	Weak positive relationship
Barnacles	0.04-0.10	Weak relationship
Hydrozoan	0.03-0.08	Weak relationship
Bryozoan	0.01-0.05	Very weak relationship

4.4 Compensation Fishing

A total of 275 compensation fishing trips were completed under the EFP, representing an estimated 8.75 km^2 of total swept area (**Table 6**). Of these, CFF scientists were onboard for 71 trips, during which 2.24 km^2 of seafloor was swept by the dredge. Total swept area across all trips was estimated by extrapolating the mean swept area per observed trip to the full fishing effort by area.

Table 6. Summary of compensation fishing effort conducted under the EFP between August 2024 and June 2026. Estimated swept area was calculated by extrapolating the mean swept area from CFF-observed trips to all compensation fishing trips within each fishing area.

Fishing Area	Time Fished	No. Trips
DBE south	Aug. - Nov. 2024	21
DBE east	Nov. 2024 - May 2025	36
RC	May 2025 - June 2026	223
Total	Aug. 2024 - June 2026	**275**

Across CFF-observed trips, data was collected from a total of 1,994 tows (482 in DBE and 1,512 in RC). Tow characteristics differed between fishing areas, with longer average tow lengths, tow times, and swept area per tow in DBE (**Table 7**). Rows with missing data were excluded from the tow statistics analysis, yielding 1,923 tows. To account for the difference in fishing effort, catch rates were standardized by swept area.

Table 7. Summary of tow level fishing effort, catch, and standardized catch per unit effort (CPUE) for CFF-observed compensation fishing trips in Davis Bank East and Rose and Crown.

	Davis Bank East	**Rose and Crown**
No. tows	482	1,441
Total swept area km^2	0.70	1.55
Mean tow length km	1.18	0.88
Mean tow time min	17.71	13.52
Mean swept area per tow km^2	0.0014	0.0011
Mean bushels per tow	14.71	16.58
Median bushels per tow	14	16
Mean CPUE bushels km^{-2}	11,004.31	18,236.46
Median CPUE bushels km^{-2}	10,268.35	15,848.50

Median tow-level CPUE was 10,268 bushels km^{-2} in DBE and 15,848 bushels km^{-2} in RC, representing a 57% higher median catch rate in the RC (**Figure 14**). Mean CPUE values showed a similar pattern (11,004 and 18,236 bushels km^{-2}, respectively). CPUE distributions differed significantly between areas (Wilcoxon rank-sum test, $W = 167{,}443$, $p < 0.001$). This difference in catch rates is consistent with the operational difficulty landing commercially viable rates in DBE described in Section 3.1.

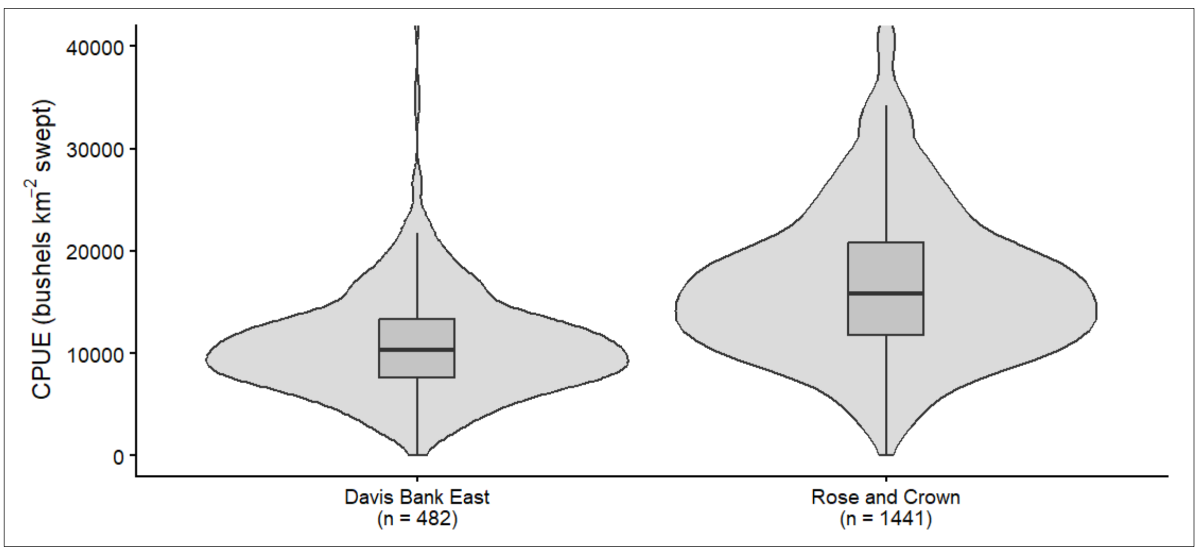

Figure 14. Tow-level catch per unit effort (CPUE) for compensation fishing trips in Davis Bank East and Rose and Crown. Violin plots show the distribution of CPUE observations, and embedded boxplot indicates the median and interquartile range.

4.4.1 Surfclam length data

Surfclam lengths were measured from a one-bushel subsample collected on 61 trips and 1,376 tows yielding 70,804 individual clam measurements. Lengths were recorded in 5 mm bins and ranged from 27-182 mm (**Figure 15a**). The size distribution was dominated by clams <120 mm and above, highlighting dredge selectivity for larger clams (Sala *et al*,. 2017). Length frequencies differed slightly between DBE and RC (**Figure 15b**).

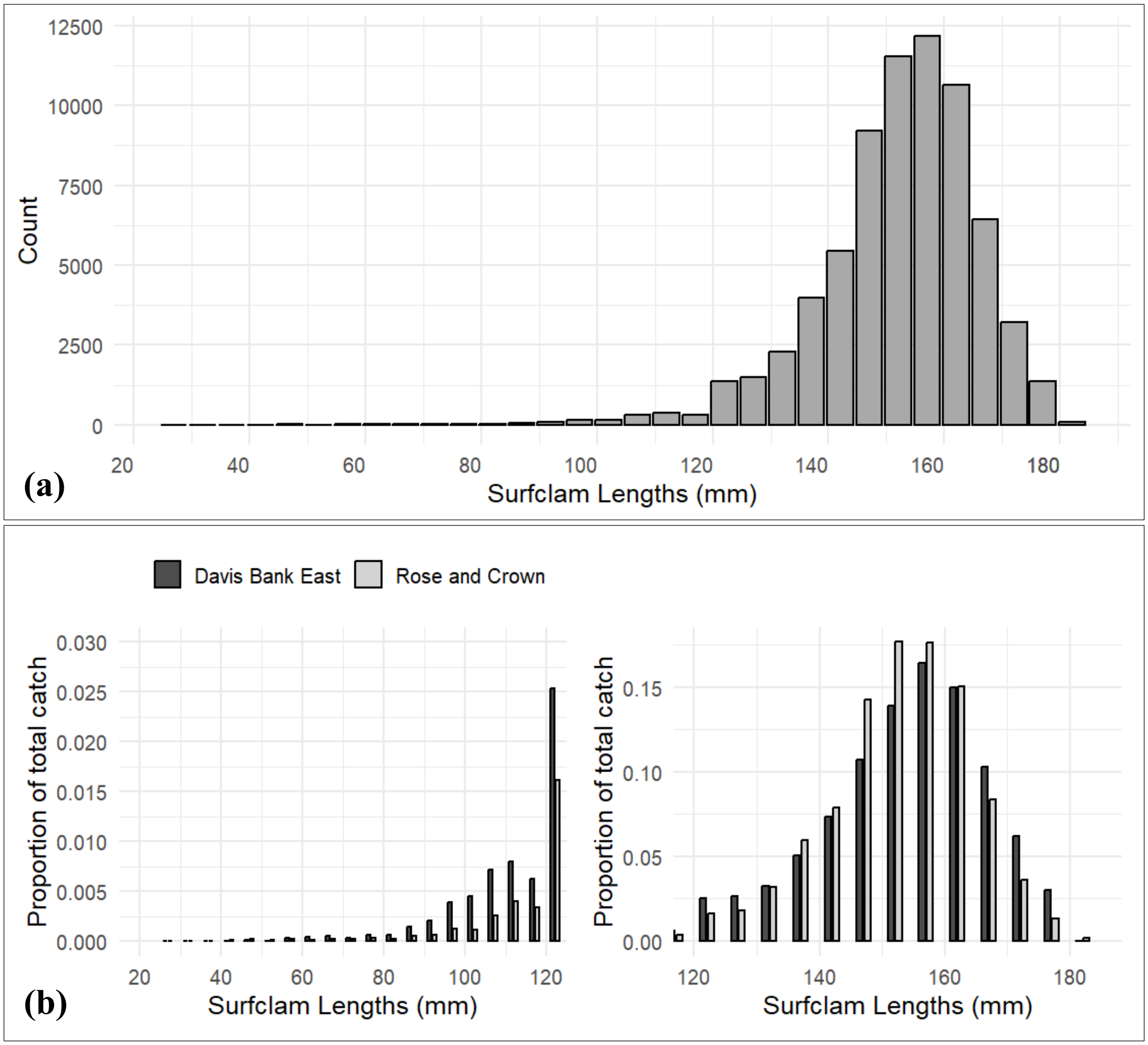

Figure 15. Surfclam length frequencies measured during CFF covered compensation fishing trips. (a) Overall length distribution of 70,804 measured clams. (b) Length frequenc1y distributions for Davis Bank East and Rose and Crown expressed as the proportion of the total catch in the area. The lower panels are split at 120 mm and are shown with two different scale values.

Clam lengths differed significantly among seasons (Kruskal-Wallis, $\chi^2 = 190.8$, $p < 0.001$; **Figure 16**). Post hoc Dunn's test indicated that all pairwise seasonal comparisons were significant (Holm-adjusted $p < 0.01$). Spring tows exhibited the smallest mean clam length (146 mm), whereas winter and fall had the largest mean lengths (153 mm). The proportion of clams ≤120 mm differed significantly among seasons (Kruskal-Wallis, $\chi^2 = 128.7$, $p < 0.001$), with summer having the highest proportion of small clams (4.7%) and spring the lowest (0.9%).

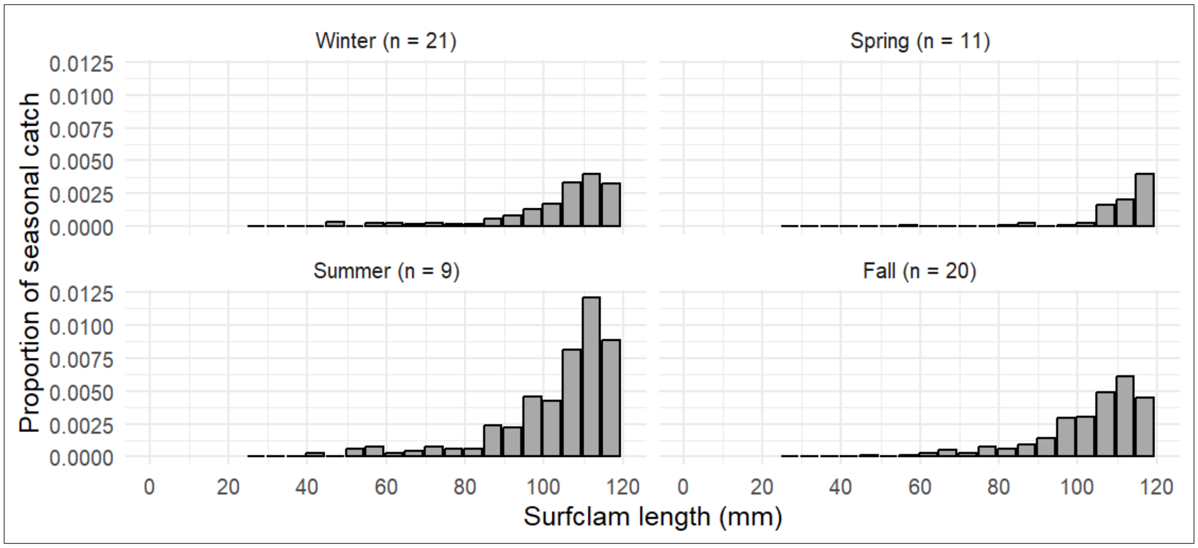

Figure 16. Seasonal length-frequency distributions of surfclams ≤120 mm. Bar heights represent the proportion of the total seasonal catch contributed by each juvenile length class. Sample size indicated the number of trips samples in each season.

4.4.2 Bycatch data

Bycatch organisms were identified from a one-bushel subsample collected for tows, with the exception of skate, finfish, and lobsters for which all individuals per tow were counted and weighed. Excluding surfclams, the most frequently observed taxa were northern moon snails (*Euspira heros*), skates, and *Cancer* spp. crabs (**Table 8**). Winter flounder (*Pseudopleuronectes americanus)* was the most common finfish bycatch, with 46 individuals recorded across 1,462 tows.

Table 8. Bycatch species and total number caught across 1,462 tows from CFF-observed compensation fishing trips.

Species	Scientific Name	Total Count	No. Subsamples
Northern moon snail	*Neverita duplicata*	1586	782
Unclassified skate	*Leucoraja ocellata* and *erinacea*	338	199
Jonah crab	*Cancer borealis*	177	124
Waved whelk	*Buccinum undatum*	173	141
Atlantic rock crab	*Cancer irroratus*	169	122
Winter flounder	*Pseudopleuronectes americanus*	46	37
Unclassified crab	*Cancer* spp.	34	23
Windowpane flounder	*Scophthalmus aquosus*	18	18

Species	Scientific Name	Total Count	No. Subsamples
American lobster	*Homarus americanus*	17	15
Monkfish	*Lophius americanus*	13	12
European flat oyster	*Ostrea edulis*	9	8
Seastar	*Asterias* spp.	5	5
Summer flounder	*Paralichthys dentatus*	5	5
Black sea bass	*Centropristis striata*	2	2
Barndoor skate	*Dipturus laevis*	2	2
Northern sea robin	*Prionotus carolinus*	1	1
Longhorn sculpin	*Myoxocephalus octodecemspinosus*	1	1

4.4.3 Productivity

Over the two-year project period, participating vessels landed approximately 107,000 bushels of surfclams during compensation fishing trips, including 24,000 bushels from DBE and 83,000 bushels from RC (GARFO- EFP Report, 6/30/2026). Assuming an average price of $30 per bushel, these landings represent an estimated $3.2 million in ex-vessel value. Extrapolated across all compensation fishing trips, approximately 2.31 km^2 of seafloor was swept in DBE and 6.44 km^2 in RC, corresponding to an estimated $312,000 and $387,000 per km^2 swept, respectively.

5. Discussion

Repeated multibeam and drop-camera observations within the DBE study area on Nantucket Shoals showed natural seasonal shifts in substrate and bathymetry consistent with high energy continental shelf environments (Blondel and Murton, 1997; Rattray *et al*., 2009). While the study area remained recognizable over two years, bathymetry, substrate composition, and habitat distribution changed substantially between surveys. Local shifts in bathymetry and backscatter showed how sediment redistribution altered the seafloor between surveys. Sandy sediments shifted to the southwest covering or exposing patches of fine pebbles that were colonized by low-succession organisms. These shifts occurred regardless of fishing exposure, indicating that large-scale natural sediment distribution was the dominant driver of physical habitat change over the study period. However, multibeam backscatter may be relatively insensitive to the subtle changes in sediment compaction and fine-scale surface roughness associated with disturbance, and sidescan sonar could potentially shoe effects from fishing activity over natural disturbance in some areas. (Legare *et al*., 2020a, 2020b). Compensation fishing in the DBE yielded approximately 24,000 bushels of Atlantic surfclams (22% of the project total), demonstrating that the area continues to support surfclam production.

Multibeam backscatter effectively distinguished sand, shell hash, and rock dominated substrates (**Figure 10**), with rock abundance as the strongest predictor of acoustic response, illustrating that backscatter is a reliable proxy for broad-scale physical habitat characterization (Le Bas and

Huvenne, 2009). Epifaunal cover did not exhibit a strong relationship with backscatter, requiring direct ground-truthing for detection. Coarse rock abundance (cobbles and boulders) contributed little additional explanatory power beyond total rock abundance, but this conclusion is constrained by the relatively homogenous rock sizes, where 98% of all measured particles larger than sand were classified as pebbles. The study area also lacked fine-grained mud, silt, clay, or detrital substrates. The limited variation in particle size likely reduced the ability to detect independent effects of coarse substrates. Evaluating these relationships in regions with a broader range of particle sizes and greater cobble and boulder occurrence could determine whether rock size becomes a driver of backscatter under different geological conditions. Similarly, conducting benthic grabs and classifying particle sizes would be an additional way to ground-truth measured particles in drop-camera images.

Sand wave movement along the seafloor within the DBE study area is characteristic of the energetic sedimentary environment of the area (Uchupi, 1968; Zeigler, 1964). The bedforms examined in this study are referred to as sand waves following previous studies of the Shoals, although they fall within the "large" and "very large" subaqueous dune classes proposed by Ashley (1990). Similar bedform activity was observed during a 2022 pilot multibeam survey of RC, where sand waves migrated approximately 10 m over a 5-month period. Bedforms migrated an average of 13 m between August 2024 and May 2025, and 21 m between May 2025 and June 2026, corresponding to an average migration rate of approximately 5.4 cm day-1. The observed southwestward migration (mean direction = 191.7°) agrees with the net sediment transport direction previously inferred from sand wave morphology and regional tidal circulation (Uchupi, 1968; Limeburner and Beardsley, 1982), showing that the seafloor is continually reworked by sediment transport. The continued migration of large bedforms means that habitat boundaries within the study area are not static and suggests that succession of epifauna associated with low-relief rocky substrate is regularly disturbed.

The physical environment of Nantucket Shoals can make distinguishing dredge-induced disturbance from natural processes inherently difficult, as turbidity generated by wind-driven waves and tidal currents regularly exceeds dredge-generated turbidity in magnitude (Tarnowski, 2006), and dredge tracks themselves are rapidly reworked by the same tidal and wave forces that reshape the surrounding seafloor (Gaspar *et al*., 2003; Tarnowski, 2006). This high-disturbance regime likely explains why epifaunal community assemblage in DBE reflects a low successional state, rather than the persistent, well-established assemblages typical of more stable hard-bottom habitats, the community is dominated by barnacles, hydrozoans, and encrusting bryozoans, taxa that are morphologically and behaviorally suited to frequent physical disturbance and rapid recolonization (Sciberras *et al*., 2013; Mercado-Allen and Goldberg, 2011). Barnacles, the most abundant epifaunal taxon, showed the strongest association with rock abundance, consistent with their dependence on stable hard substrate for settlement and their capacity to feed effectively even under strong tidal flow (LaBarbera, 1977; Crisp, 1960; Bertness *et al*., 1991); evidence of barnacle scour (**Figure A1c**) further reflects the high-flow, physically disturbed regime characteristic of this setting (Powell *et al*., 2020). Hydrozoans and encrusting bryozoans, while similarly dependent on hard substrate, showed less resilience to this disturbance regime, hydrozoan cover declined markedly between surveys, plausibly reflecting burial and re-exposure of colonies during periods of active sediment transport (Sheehan *et al*., 2013, **Figure A1d**) compounded by seasonal changes in wave energy and food availability (Winder and Cloern, 2010), while encrusting bryozoans remained in comparatively low abundance throughout the study period.

The study area in DBE experienced approximately six months of fishing pressure (51 trips) before fishing operations moved to RC. Although the duration of fishing within DBE was relatively short and fishing exposure could only be quantified using a subset of observed tow tracks, localized biological responses were detected. Bryozoan cover declined significantly with increasing fishing exposure, while longitudinal analyses indicated that hydroid cover also decreased over time at stations closer to observed tow tracks. Encrusting bryozoan are common suspension feeders that colonize hard substrates and compete directly with other sessile organisms for attachment space (McKinney and Jackson, 1989). Their dependence on exposed substrate makes them particularly susceptible to burial, scour, and physical abrasion and are often considered indicators of disturbance in hard-bottom benthic environments. Unlike habitat-forming bryozoans, the encrusting bryozoans observed in this study contribute little structural complexity and are therefore unlikely to provide substantial ecological benefits to the biota of the region.

Another perspective of the impacts of bottom-tending fishing gears is that periodic dredging may increase productivity of organisms like surfclams by reducing overcrowding and increasing food availability (*pers. comm.* with surfclam fishermen familiar with the area). While this hypothesis is very difficult to test, fishermen's continued preference for historically productive fishing grounds was evident during compensation fishing. After fishing effort was relocated to RC, vessels were permitted to fish throughout a 69 km^2 area, yet captains consistently returned to the same general region previously fished under EFP 19066 (**Figure A2**). Approximately 40,000 bushels of surfclams were landed under EFP 19066 in 104 fishing trips and continued targeting of the same grounds suggests that fishermen perceive this area to remain among the most productive surfclam habitat available to them in the GSC HMA. The abundance of shell hash and shell fragments (**Figure A1e and A1f**) throughout the study area may contribute to the continued productivity of these fishing grounds. Shell material provides structural complexity, serves as refuge for newly settled juveniles, buffers sediment chemistry, and creates attachment surfaces (Gutiérrez *et al*., 2003; Kraeuter *et al*., 2003; Parsons-Hubbard *et al*., 2001). These functions may help support both continued surfclam recruitment and the epifaunal communities associated with shell-rich substrates observed in this study. The persistence of shell-rich habitats therefore likely supports continued recruitment in addition to providing suitable habitat for adult surfclams.

Approximately 25% of EFP 23073 compensation fishing trips were accompanied by CFF scientists, providing a fine-scale record of fishing activity and habitat interactions that are rarely available for the federal surfclam fishery. Observed bycatch during compensation fishing remained low across all monitored trips (**Table 8**). Most one-bushel subsamples contained few non-target organisms, with catches dominated by naturally abundant species such as moon snails and only occasional occurrences of skate and fish species. Beyond generating these observations, the compensation fishing program was the source of research funds for the repeated benthic habitat surveys conducted throughout the project. Together, the combination of fishermen's local ecological knowledge, targeted scientific observations, and repeated habitat surveys provided an opportunity to evaluate commercial surfclam fishing within a managed habitat area.

These results have direct relevance to the management of the GSC HMA. The widespread changes in substrate observed throughout the study area, regardless of fishing intensity, suggest that natural sediment redistribution was the primary driver of physical habitat dynamics during the study period. This conclusion would be strengthened by a more robust comparison between areas of seafloor known to be fished and unfished. Epifaunal communities exhibited localized responses associated with fishing exposure, particularly bryozoans, suggesting that these biological communities may provide a more sensitive indicator of fishing effects than substrate alone. The consistently higher catch rates observed in RC relative to DBE (Section 4.4) likely reflect differences in surfclam density, substrate, or accessibility between the two areas, and warrant further investigation given their direct influence on where compensation fishing effort was ultimately concentrated. The persistence of productive Atlantic surfclam populations within this physically disturbed setting is itself consistent with the species known tolerance of frequent natural disturbance (Fay *et al*., 1983; Cargnelli *et al*., 1999), though distinguishing natural from fishing-related habitat variability will continue to require repeated, multi-year monitoring rather than single observations (Brown *et al*., 2011). This study demonstrates the practical value of pairing acoustic mapping with optical ground-truthing, collected in partnership with the commercial surfclam fleet, as a cost-effective long-term framework for assessing habitat conditions and informing management decisions within the GSC HMA.

6. Future Work

This study provides a robust framework for evaluating habitat dynamics within the DBE area and a foundation for continued directed monitoring. The original study design proposed a baseline survey of the full study area followed by compensation fishing in one polygon while repeated habitat surveys continued in the other, with a final full-area survey directly evaluating habitat vulnerability and recovery. However, compensation fishing effort shifted to RC requiring the survey design to adapt accordingly. As a result, this study provides insight into habitat variability and localized fishing effects but could not directly quantify rates of habitat recovery following disturbance. Future research incorporating repeated surveys immediately before and after fishing events would provide a stronger framework for quantifying habitat vulnerability, recovery, and the persistence of fishing-related changes within these naturally dynamic environments. Future surveys targeting areas within the GSC HMA that contain benthic habitats underrepresented in DBE, such as extensive cobble fields, boulder habitat, and mussel beds, would broaden the range of substrate types available for analysis. Expanding habitat coverage would improve understanding of backscatter-habitat relationships, assess whether rock size becomes a stronger predictor of backscatter where coarse substrates are more common, and allow evaluation of fishing effects across a wider range of benthic environments. Additional sediment classification with benthic grab sampling in these areas would provide an independent means of ground-truthing rock sizes. Incorporating higher-resolution acoustic methods, such as side-scan sonar, alongside multibeam surveys would further improve detection of subtle changes in sediment compaction, surface roughness, and dredge tracks that may not be fully resolved using multibeam backscatter alone. Together, these approaches would strengthen future assessments of habitat dynamics and fishing-related disturbance on Nantucket Shoals.

7. Literature Cited

Ashley, G. M. 1990. Classification of large-scale subaqueous bedforms: a new look at an old problem. Journal of Sedimentary Research 60:160-172.

Auster, P. J., R. J. Malatesta, C. L. S. Donaldson, R. W. Langton, L. Watling, P. C. Valentine, C. L. S. Donaldson, E. W. Langton, A. N. Shepard, and I. G. Babb. 1995. The impacts of mobile fishing gear on seafloor habitats in the Gulf of Maine (Northwest Atlantic): implications for conservation of fish populations. Reviews in Fisheries Science 3:185-202.

Bertness, M. D., Gaines, S. D., Bermudez, D., & Sanford, E. 1991. Extreme spatial variation in the growth and reproductive output of the acorn barnacle Semibalanus balanoides. Marine Ecology Progress Series, 75, 91-100.

Blondel, P., and B. J. Murton. 1997. Handbook of seafloor sonar imagery. Wiley-Praxis.

Boero, F. 1984. The ecology of marine hydroids and effects of environmental factors: A review. Marine Ecology, 5(2), 93-118.

Brown, C. J., S. J. Smith, P. Lawton, and J. T. Anderson. 2011. Benthic habitat mapping: a review of progress towards improved understanding of the spatial ecology of the seafloor using acoustic techniques. Estuarine, Coastal and Shelf Science 92:502-520.

Cargnelli, L. M., S. J. Griesbach, D. B. Packer, and E. Weissberger. 1999. Essential Fish Habitat Source Document: Atlantic Surfclam, Spisula solidissima, Life History and Habitat Characteristics. NOAA Technical Memorandum NMFS-NE-142.

Collier, J. S., and C. J. Brown. 2005. Correlation of sidescan backscatter with grain size distribution of surficial seabed sediments. Marine Geology 214:431-449.

Crisp, D. J. 1960. Factors influencing growth rate in barnacles. Journal of Animal Ecology 29:95-116.

Diaz, R. J., M. Solan, and R. M. Valente. 2004. A review of approaches for classifying benthic habitats and evaluating habitat quality. Journal of Environmental Management 73:165-181.

Eigaard, O. R., Bastardie, F., Breen, M., Dinesen, G. E., Hintzen, N. T., Laffargue, P., Mortensen, L. O., Nielsen, J. R., Nilsson, Hans C., O'Neill, F. G., Polet, H., Reid, David G., Sala, A., Sko¨ld, M., Smith, C., Sørensen, T. K., Tully, O., Zengin, M., and Rijnsdorp, A. D. 2016. Estimating seabed pressure from demersal trawls, seines, and dredges based on gear design and dimensions. ICES Journal of Marine Science 73:27-43.

Eigaard, O. R., Bastardie, F., Hintzen, N. T., Buhl-Mortensen, L., Buhl-Mortensen., P., Catarino, R., Dinesen, G. E. Egekvist, J., Fock, H. O., Geitner, K., Gerritsen, H. D., Gonzalez, M. M., Jonsson, P., Kavadas, S., Laffargue, P., Lundy, M., et al. 2017. The footprint of bottom trawling in European waters: distribution, intensity, and seabed integrity. ICES Journal of Marine Science, 74:847-865.

Fay, R. R., R. J. Neves, and G. B. Pardue. 1983. Species profiles: life histories and environmental requirements of coastal fishes and invertebrates (North Atlantic)-surf clam. U.S. Fish and Wildlife Service FWS/OBS-82/11.13.

Fewings, M. R., and S. J. Lentz. 2011. Summertime cooling of the shallow continental shelf. Journal of Geophysical Research 116:C07015.

Gaspar, M. B., Leitao, F., Santos, M. N., Chicaro, L., Dias, M. D., Chicaro, A., and C. C. Monteiro. 2003. A comparison of direct macrofaunal mortality using three types of clam dredges. ICES Journal of Marine Science 60:733-742.

Greenberg, D. A. 1983. Modeling the mean barotropic circulation in the Bay of Fundy and Gulf of Maine. Journal of Physical Oceanography 13:886-904.

Gutiérrez J. L., C. G. Jones, D. L. Strayer, and O. O. Iribarne. 2003. Mollusks as ecosystem engineers: the role of shell production in aquatic habitats. Oikos 101:79-90.

Harris, B. P., Cowles, G. W., & Stokesbury, K. D. E. 2012. Surficial sediment stability on Georges Bank, in the Great South Channel and on eastern Nantucket Shoals. Continental Shelf Research 49:65-72.

Jennings, N., Garcia, L., Davis, F., and R. Munnelly. 2022. Great South Channel Habitat Management Area Survey, Final Report for Exempted Fishing Permit #19066. (https://s3.us-east-1.amazonaws.com/nefmc.org/6.-CFF-PR-EFP19066-Feb2022.pdf)

Jones, N. S., Thompson, I., and W. Ambrose. 1978. Age and growth rate determinations for the Atlantic surf clam, Spisula solidissima (Bivalvia:Mactracea), based on internal growth lines on shell cross-sections. Marine Biology 47:63-70.

Kenny, A. J., Cato, I., Desprez, M., Fader, G., Shuttenhelm, R. T. E., and J. Side. 2003. An overview of seabed mapping technologies in the context of marine habitat classification. ICES Journal of Marine Science 60:411-418.

Kostylev, V. E., Todd, B. J., Fader, G. B., Courtney, R. C., Cameron, G. D. M., and R. A. Pickrill. 2001. Benthic habitat mapping on the Scotian Shelf based on multibeam bathymetry, surficial geology and sea floor photographs. Marine Ecology Progress Series 219:121-137.

Kraeuter, J. N., M. J. Kennish, J. Dobarro, S. R. Fegley and G. E. Flimlin, Jr. 2003. Rehabilitation of the northern quahog (hard clam) (Mercenaria mercenaria) habitat by shelling-11 years in Barnegat Bay, New Jersey. J. Shellfish Res. 22:61-67.

LaBarbera, M. (1977). Brachiopod orientation to water movement. Theory, laboratory behavior and field observations. Paleobiology, 3:270-287.

Le Bas, T. P., and V. A. I. Huvenne. 2009. Acquisition and processing of backscatter data for habitat mapping-Comparison of multibeam and sidescan systems. Applied Acoustics 70(10):1242-1247.

Legare, B. J., Nichols, O. C., and M. Borrelli. 2020a. Persistence of hydraulic dredge tracks following surfclam harvesting in shallow water. Journal of Shellfish 39:331-336.
Legare, B. J., Mittermayr, A., and M. Borrelli. 2020b. The impacts of hydraulic clamming in shallow water and importance of incorporating anthropogenic disturbances into habitat assessments. Aquatic Living Resources 33:13.

Limeburner, R., and R. C. Beardsley. 1982. The seasonal circulation of the Gulf of Maine. Journal of Physical Oceanography 13:2187-2206.

McGonigle C., Brown, C. J., Quinn, R., and J. Grabowski. 2009. Evaluation of image-based multibeam sonar backscatter classification for benthic habitat discrimination and mapping at Stanton Banks, UK. Estuarine, Coastal and Shelf Science 81(3):423-437.

McKinney, F. K., and J. B. C. Jackson. 1989. Bryozoan Evolution. University of Chicago Press.

Mercado-Allen, R., and R. Goldberg. 2011. Review of the ecological effects of dredging in the cultivation and harvest of molluscan shellfish NOAA Technical Memorandum NMFS-NE-220.

Munroe, D. M., Powell, E. N., Mann, R., Klinck, J. M., and E. E. Hofmann. 2013. Underestimation of primary productivity on continental shelves: Evidence from maximum size of extant surfclam (Spisula solidissima) populations. Fisheries Oceanography 22:220-233.

Nishizaki, M. T., and E. Carrington. 2015. The effect of water temperature and velocity on barnacle growth: Quantifying the impact of multiple environmental stressors. Journal of Thermal Biology 54:37-46.

Okamura, B. 1987. Particle-size and flow velocity induce an inferred switch in bryozoan suspension-feeding behaviour. Biological Bulletin (Woods Hole) 173: 222-229.

Parsons-Hubbard, K. M., E. N. Powell, G. M. Staff, W. R. Callender, C. E. Brett, and S. E. Walker. 2001. The effect of burial on shell preservation and epibiont cover in Gulf of Mexico and Bahamas shelf and slope environments after two years: an experimental approach. In: J. Y. Aller, S. A. Woodin, and R. C. Aller (eds.), Organism-Sediment Interactions pp297-314.

Powell, E. N., Mann, R. L., Long, M. C., Timbs, J. R., and K. M. Kuykendall. 2021. The conundrum of biont-free substrates on a high-energy continental shelf: Burial and scour on Nantucket Shoals. Estuarine, Coastal and Shelf Science 249:107089.

R Core Team. 2025. R: A Language and Environment for Statistical Computing. R Foundation for Statistical Computing, Vienna, Austria.

Rattray, A., Ierodiaconou, D., Laurenson, L., Burq, S., and M. Reston. 2009. Hydro-acoustic remote sensing of benthic biological communities on the shallow South East Australian continental shelf. Estuarine, Coastal and Shelf Science 84: 237-245.

Ruffin, K. K. 1995. The effects of hydraulic clam dredging on nearshore turbidity and light attenuation in Chesapeake Bay, MD. Master's Thesis, University of Maryland. 79pp.

Scibberas, M., Hinz, H., Bennell, J. D., Jenkins, S. R., Hawkins, S. J., and M. J. Kaiser. 2013. Benthic community response to a scallop dredging closure within a dynamic seabed habitat. Marine Ecology Progress Series 480:83-98.

Sheehan, E. V., Cousens, S. L., Nancollas, S. J., Stauss, C., Royle, J., and M.J. Attrill. 2013. Drawing lines at the sand: Evidence for functional vs. visual reef boundaries in temperate Marine Protected Areas. Marine Pollution Bulletin 76:194-202.

Soulsby, R. L. 1997. Dynamics of Marine Sands. Thomas Telford Publications, London.

Sousa, W. P. 1984. The role of disturbance in natural communities. Annual Review of Ecology and Systematics 15:353-391.

Tarnowski, M. 2006. Maryland's coastal shellfish monitoring report. (Verify report title.)

Trygonis, V., and M. Sini. 2012. PhotoQuad: A dedicated seabed image processing software, and a comparative error analysis of four photoquadrat methods. Journal of Experimental Marine Biology and Ecology 425: 99-108.

Twitchell, D. C. 1983. Bedform distribution and inferred sand transport on Georges Bank, United States Atlantic continental shelf. Sedimentology 30: 695-710.

Uchupi, E. 1968. Atlantic Continental Shelf and Slope of the United States-Physiography. U.S. Geological Survey Professional Paper 529-C.

Wentworth, C. K. 1922. A grade scale and class terms for clastic sediments. Journal of Geology 30:377-392.

Winder, M., and J. E. Cloern. 2010. The annual cycles of phytoplankton biomass. Journal of Plankton Research 32:1145-1158.

Ziegler, J. M., Tuitle, S. D., Tasha, H. J., and G. S. Geise. 1964. Pleistocene geology of outer Cape Cod. Bulletin Geology. SOCA. m., 75:705-714.

8. Appendix

This appendix contains supplementary tables and figures that support the methods, results, and discussion presented in the main report.

Table A1. Species library used in *PhotoQuad* to define the substrate and epifaunal categories available for annotation.

Species name	Species ID	Group Name	Group ID
Sand	1	Sand	1
Sand ripples	2	Sand	1
Sand dune	3	Sand	1
Sand and small shell hash	4	Sand	1
Rock	5	Rock	2
Rock with encrusting bryozoan	6	Rock	2
Rock with barnacles	7	Rock	2
Rock with hydroid	8	Rock	2
Clam shell	9	Shell	3
Clam shell with encrusting bryozoan	10	Shell	3
Clam shell with barnacles	11	Shell	3
Clam shell with hydroid	12	Shell	3
Mussel shell	13	Shell	3
Mussel shell with encrusting bryozoan	14	Shell	3
Mussel shell with barnacles	15	Shell	3
Mussel shell with hydroid	16	Shell	3
Other shell	17	Shell	3
Other shell with encrusting bryozoan	18	Shell	3
Other shell with barnacles	19	Shell	3
Other shell with hydroid	20	Shell	3
Hydroid	21	Epifauna	4
Live mussel	22	Epifauna	4
Live mussel with encrusting bryozoan	23	Epifauna	4

Live mussel with barnacles	24	Epifauna	4
Live mussel with hydroid	25	Epifauna	4
Encrusting bryozoan	26	Epifauna	4
Barnacles	27	Epifauna	4
Algae	28	Epifauna	4
Unknown sponge	29	Epifauna	4
Mud/silt	30	Mud	5
Unknown item	31	Unknown	6
Cancer crab	32	Megafauna	7
Skate spp	33	Megafauna	7
Fish spp	34	Megafauna	7
Moonsnail	35	Megafauna	7

Table A2. Still image point annotations by category sorted by most commonly annotated to least across four drop-camera surveys in the Davis Bank East study area.

Point Designation	**Aug2024**	**Sept2024**	**May2025**	**June2026**	**Total**
Sand	4906	3255	4248	5123	17532
Plus small shell hash	2705	3038	2187	2815	10745
Rock	1785	2098	2073	1531	7487
Rock with hydroid	108	660	269	65	1102
Rock with barnacles	81	279	483	247	1090
Clam shell	105	188	125	58	476
Mussel shell	53	78	88	35	254
Clam shell with hydroid	28	74	42	18	162
Rock with encrusting bryozoan	16	65	38	1	120
Mussel shell with barnacles	2	32	63	20	117
Clam shell with barnacles	14	24	52	16	106
Other shell	8	5	49	29	91
Mussel shell with hydroid	11	36	32	2	81

Live mussel with hydroid	3	38	32		73
Hydroid	6	11	53	3	73
Live mussel with barnacles	16	31	13	11	71
Other shell with hydroid	5	7	44	8	64
Other shell with barnacles		1	54	7	62
Clam shell with encrusting bryozoan	1	42	12	1	56
Sand ripples	42				42
Mussel shell with encrusting bryozoan	1	16	14	1	32
Other shell with encrusting bryozoan	1	7	10	3	21
Live mussel with encrusting bryozoan	2	7	5	1	15
Sand dune		2	10	3	15
Algae		3		2	5
Live mussel	1	3			4
Cancer crab			1		1
Man-made item			1		1
Moonsnail			1		1
Scallop seed			1		1
Grand Total	9900	10000	10000	10000	39900

Table A3. Full list of habitat metrics tested in the backscatter-habitat prediction analysis.

Habitat Metrics by Station
Depth_m
Granule_n
Pebble_n
Cobble_n
Boulder_n
Mean_size
Max_size

TotalRock_n
Fine_n
Coarse_n
Hydroid_cover
Barnacle_cover
Bryozoan_cover
Total_epifauna_cover
ShellHash_pts
MusselShell_pts
ClamShell_pts
OtherShell_pts
Total_shell_pts
Sand_pts
SandRipple_pts
SandDune_pts
Total_sand_pts

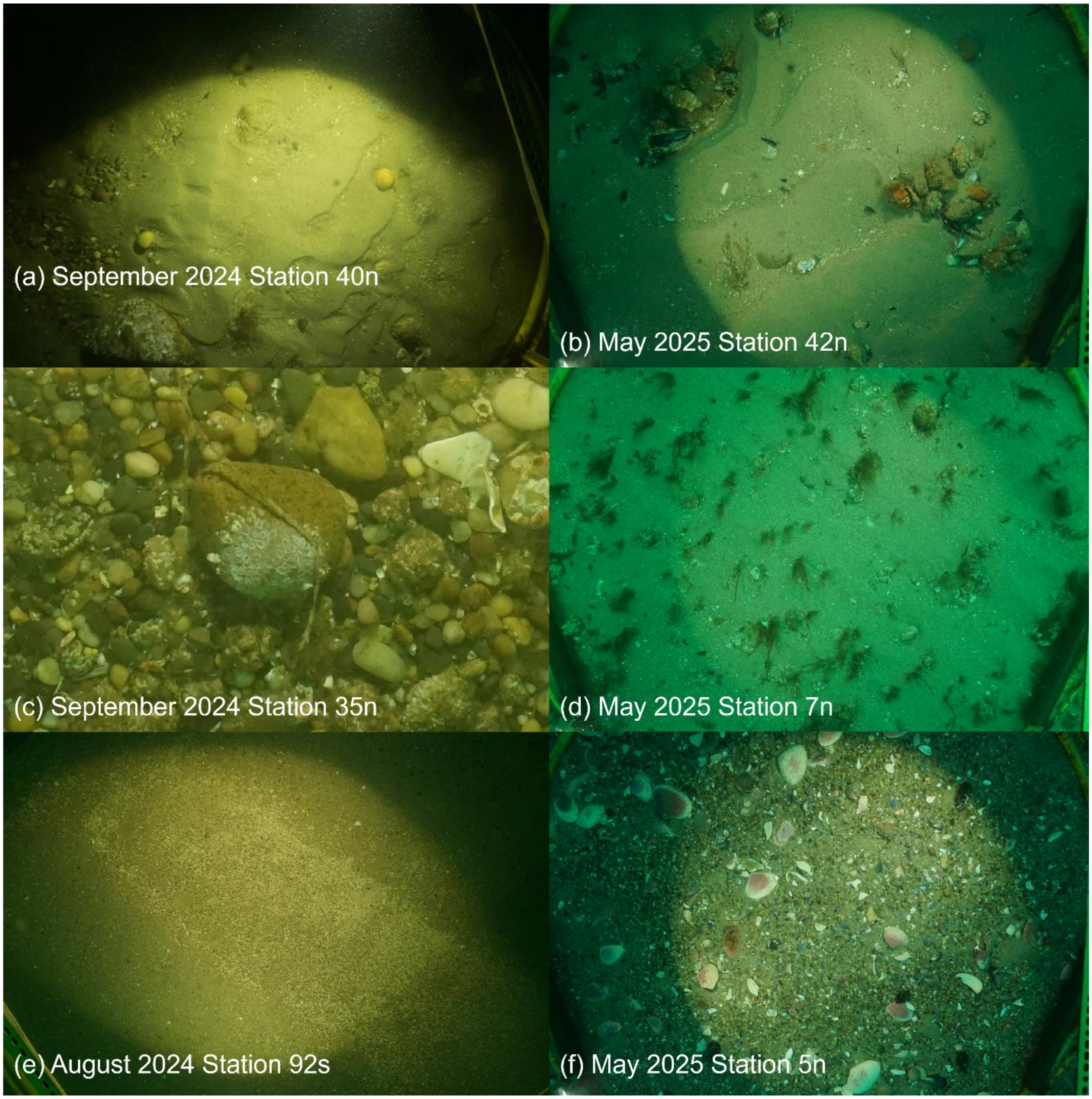

Figure A1. Select images from drop-camera surveys illustrating habitat characteristics including (a) the singular occurrence of a rock classified as a boulder across four surveys, (b) mussel occurrence with epifaunal growth, (c) barnacle scour, (d) hydrozoan growth with hard surfaces buried by sand, and (e) and (f) shell hash and shell fragments.

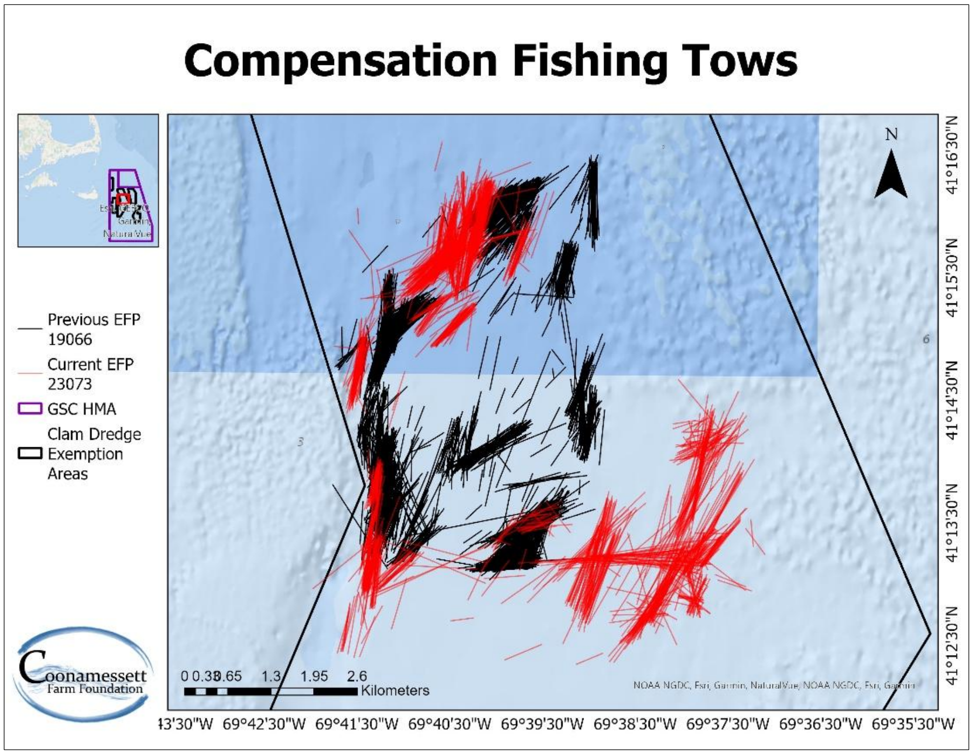

Figure A2. Compensation fishing tow tracks within the Rose and Crown research area. Red lines show tow tracks completed on CFF-observed trips under the current EFP 23073 (2024-2026); black lines show tow tracks completed under EFP 19066 (2020-2022; Jennings *et al*., 2022).